# Climatological Aspects of Mesoscale Cyclogenesis over the Ross Sea and Ross Ice Shelf Regions of Antarctica*

JORGE F. CARRASCO† AND DAVID H. BROMWICH

*Polar Meteorology Group, Byrd Polar Research Center and Atmospheric Sciences Program, The Ohio State University, Columbus, Ohio*

(Manuscript received 26 October 1993, in final form 8 April 1994)

ABSTRACT

A one-year (1988) statistical study of mesoscale cyclogenesis near Terra Nova Bay and Byrd Glacier, Antarctica, was conducted using high-resolution digital satellite imagery and automatic weather station data. Results indicate that on average two (one) mesoscale cyclones form near Terra Nova Bay (Byrd Glacier) each week, confirming these two locations as mesoscale cyclogenesis areas. The maximum (minimum) weekly frequency of mesoscale cyclones occurred during the summer (winter). The satellite survey of mesoscale vortices was extended over the Ross Sea and Ross Ice Shelf. Results suggest southern Marie Byrd Land as another area of mesoscale cyclone formation. Also, frequent mesoscale cyclonic activity was noted over the Ross Sea and Ross Ice Shelf, where, on average, six and three mesoscale vortices were observed each week, respectively, with maximum (minimum) frequency during summer (winter) in both regions. The majority (70%–80%) of the vortices were of comma-cloud type and were shallow. Only around 10% of the vortices near Terra Nova Bay and Byrd Glacier were classified as deep vortices, while over the Ross Sea and Ross Ice Shelf around 20% were found to be deep.

The average large-scale pattern associated with cyclogenesis days near Terra Nova Bay suggests a slight decrease in the sea level pressure and 500-hPa geopotential height to the northwest of this area with respect to the annual average. This may be an indication of the average position of synoptic-scale cyclones entering the Ross Sea region. Comparison with a similar study but for 1984–85 shows that the overall mesoscale cyclogenesis activity was similar during the three years, but 1985 was found to be the year with greater occurrence of "significant" mesoscale cyclones. The large-scale pattern indicates that this greater activity is related to a deeper circumpolar trough and 500-hPa polar vortex for 1985 in comparison to 1984 and 1988. This means that 1985 had more frequent and/or stronger warm air advection toward the Ross Sea area caused by synoptic-scale cyclones decaying near Marie Byrd Land and had more frequent and/or stronger cold katabatic air outbreaks from East Antarctica onto the southwestern corner of the Ross Sea. The convergence of these two air masses creates boundary layer baroclinic zones that can undergo mesoscale cyclogenesis.

## 1. Introduction

Studies of synoptic-scale cyclogenesis over the Southern Hemisphere (e.g., Taljaard 1967; Trenberth 1991) indicate that it occurs frequently in midlatitudes, but it is infrequent near the coast of Antarctica. Moreover, trajectories of the synoptic-scale storms revealed that the oceans adjacent to the Antarctic continent are cyclolysis areas for these features (Streten and Troup 1973; Carleton 1979). This is reflected in the broad-scale climatology of the high southern latitudes that shows four quasi-stationary synoptic-scale low pressure centers around the Antarctic continent. One of these is located to the north of the Marie Byrd Land–Ross Ice Shelf region giving a semipermanent cyclonic circulation over the area (Fig. 1) (Schwerdtfeger 1970, 1984). Although cyclogenesis is considered infrequent in the circumpolar trough (Schwerdtfeger 1984), observational satellite studies (Carleton 1981a,b, 1983; Carleton and Carpenter 1989, 1990; Shanmin et al. 1990) have shown that it takes place on the west side of synoptic-scale cyclones decaying near Antarctica. This cyclogenesis mainly occurs on the subsynoptic scale (100–500 km; Carleton and Fitch 1993) and is associated with cold polar air advected by southerly winds into the much warmer and moister environment over the ocean.

Recent studies (Bromwich 1991; Carleton and Carpenter 1990; Carleton and Fitch 1993; Fitch and Carleton 1992; Heinemann 1990; Turner and Thomas 1992; Warren and Turner 1989; Carrasco 1992; Carrasco and Bromwich 1991, 1992, 1993a,b; Turner et al. 1993a) have demonstrated that the Antarctic coastal areas as well as the surrounding sea-ice zone are active regions for subsynoptic-scale cyclone development. Because of

* Contribution 906 of Byrd Polar Research Center.

† Permanent affiliation: Dirección Meteorológica de Chile, Santiago, Chile.

*Corresponding author address:* Dr. David H. Bromwich, The Ohio State University, Byrd Polar Research Center, 1090 Carmack Road, Columbus, OH 43210-1002.

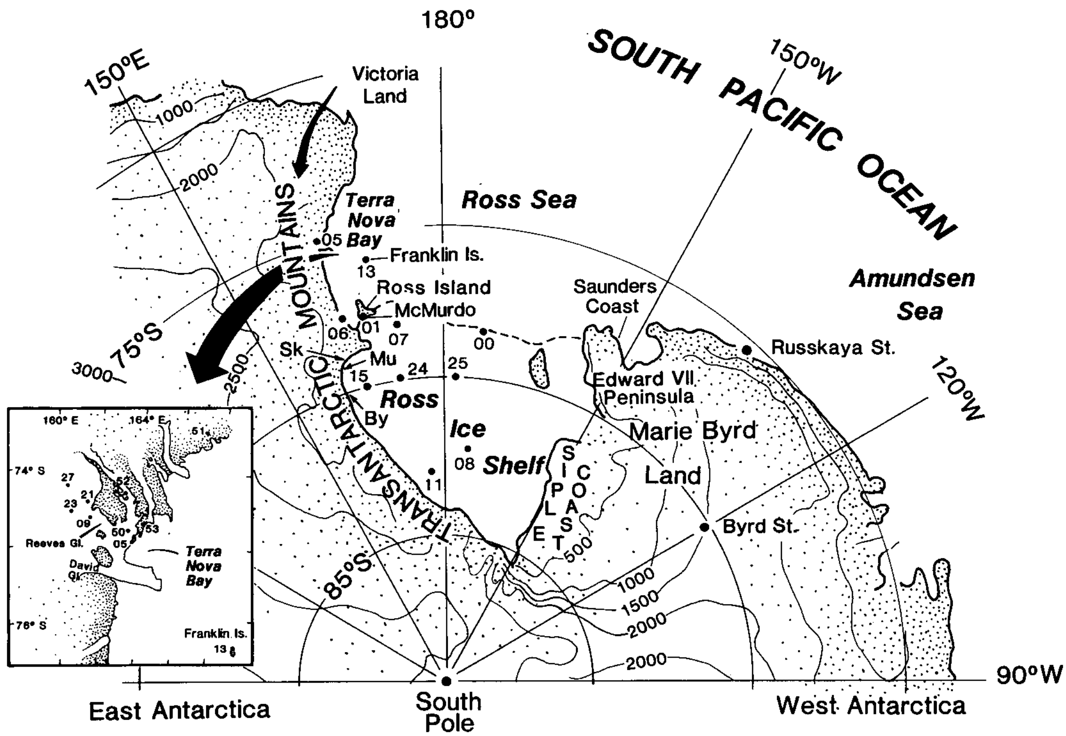


FIG. 1. Location map of the Ross Sea, Ross Ice Shelf, and Victoria Land areas. The numbered dots are AWS sites. Here, Sk, Mu, and By denote Skelton, Mulock, and Byrd Glaciers, respectively.

their characteristics these disturbances have been classified as "polar lows." This term, originally used by British meteorologists to refer to cold air depressions, was defined by Businger and Reed (1989) as any type of subsynoptic-scale cyclone that develops within a cold air mass poleward of major jet streams or frontal zones and whose main cloud is largely of convective origin. Mansfield (1974) restricted the use of polar lows to shallow disturbances growing entirely within the polar air mass excluding the type of system that develops behind the frontal zone typically associated with an upper-level jet [classified as short wave–jet streak type by Businger and Reed (1989)]. In this article, mesoscale cyclone or vortex is used to refer to all cyclonic perturbations whose diameters are less than $10^3$ km and that develop within the cold air environment of Antarctica and the surrounding sea-ice–ocean areas.

Parish and Bromwich (1987, 1991) simulated the near-surface wind regime over the Antarctic continent. Their results show that the winds converge into several zones near the coastal margin of the continent. In these confluence zones, cooled near-surface air descends from the high plateau (katabatic winds) and blows in an intensified and persistent fashion away from the foot of the coastal slopes. One of these zones is located inland of Terra Nova Bay (Figs. 1 and 2), where the intense katabatic winds that descend through Reeves and David Glaciers blow out onto the southwestern Ross Sea, sometimes reaching the area around Franklin Island (Bromwich 1986, 1989a; Bromwich et al. 1990; Parish and Bromwich 1989). A boundary layer baroclinic zone can form when a cold jet of continental air invades the warmer maritime air located over the southwestern corner of the Ross Sea. This feature, in conjunction with a weak surface trough, constitutes sufficient conditions for mesoscale cyclogenesis (Bromwich 1989b).

Bromwich (1991) used two years of automatic weather station (AWS) observations and hard-copy DMSP (Defense Meteorological Satellite Program) satellite images of 2.7-km resolution to study mesoscale cyclogenesis along the Transantarctic Mountains and found that in the region adjacent to Terra Nova Bay mesoscale cyclones form with great frequency. One or two mesoscale vortices formed each week during the period studied (1984–85). Also, individual case studies (Bromwich 1987, 1989b, 1991; Carrasco and Bromwich 1991, 1993a) revealed that katabatic outflows play an important role in the formation of these mesoscale cyclones. The same conditions occur with lower frequency over the northwestern side of the Ross Ice Shelf. In this case, the establishment of a boundary layer baroclinic zone is linked to the intensified transport of cold katabatic air coming from East Antarctica through Byrd

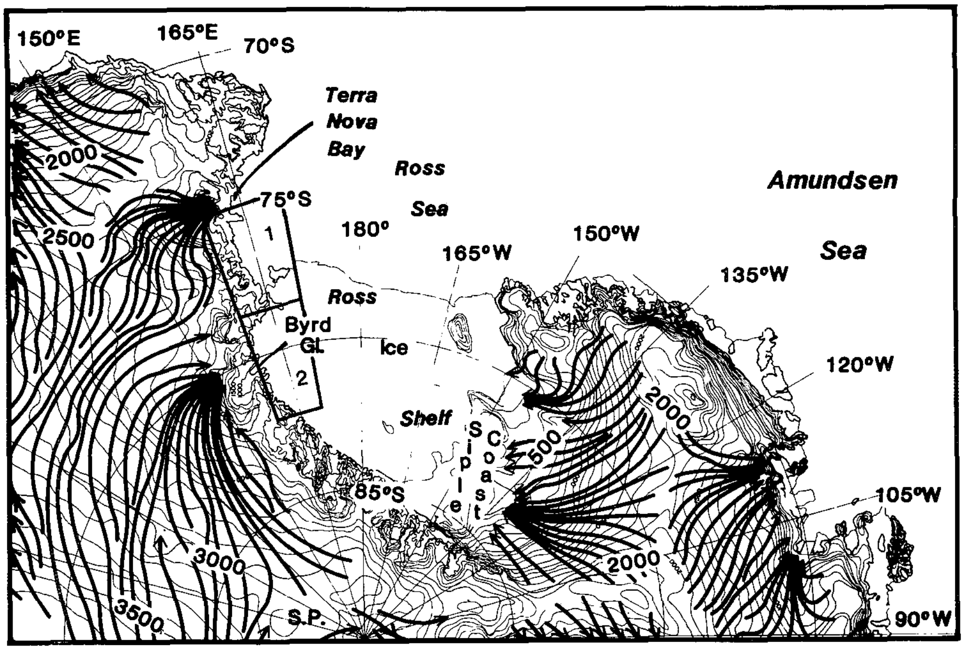


FIG. 2. Partial reproduction of the simulated streamlines of time-averaged surface winds over Antarctica (heavy lines) from Parish and Bromwich (1987) with cyclogenetic areas marked from Bromwich (1991): 1) Terra Nova Bay–Franklin Island area and 2) Byrd Glacier area. Thin lines are elevation contours in 100-m increments.

Glacier (Parish and Bromwich 1987; Bromwich 1989c).

The role of mesoscale cyclones in the regional and broadscale climatology of the high southern latitudes is not completely understood and needs further investigation. It has been suggested that they can contribute in part to the precipitation over the coastal slopes of the continent (Tzeng et al. 1993; Carrasco and Bromwich 1993a). Their interaction with the synoptic-scale circulation was demonstrated by Bromwich (1989b), who studied a mesoscale cyclone that developed into a synoptic-scale feature, and by Carrasco and Bromwich (1993a), who studied a case where a mesoscale cyclone underwent significant development when supported by the broadscale circulation. Also, O'Connor et al. (1994) found that mesoscale cyclones passing to the east of Ross Island can generate barrier winds along the Transantarctic Mountains near Ross Island, resulting in gale-force winds at McMurdo Station. In general, James (1989) suggested that mesoscale cyclones frequently forming around the edge of Antarctica may be one of the mechanisms that could weaken the polar vortex by extracting energy from it and allowing the persistence of the drainage flow and/or its reestablishment. Although he concluded that this is unlikely because mesoscale cyclone formation and development take place below 700 hPa (which is below the summit of the ice sheet), there is not a reliable climatology of these features to see whether or not they contribute significantly to the vorticity balance of the Antarctic troposphere. In addition, a recent general circulation modeling study by Murray and Simmonds (1991) found a high-latitude maximum of cyclones that may be associated with mesoscale cyclogenesis that takes place near the Antarctic coastline. In another climate model study, Tzeng et al. (1993) resolved a subpolar convergence zone that may be related to mesoscale cyclone activity.

The above implies that in spite of the growing appreciation of the importance of mesoscale cyclones in high southern latitudes, there is a need to more accurately define their frequency and characteristics, to precisely determine the climatic role of these cyclones and their interaction with synoptic-scale features, and to investigate the dynamical processes involved in their formation, development, and lysis. This article presents a one-year study of mesoscale cyclogenesis near Terra Nova Bay/Franklin Island and Byrd Glacier (Fig. 2). The selection of the year was based solely on the availability of digital satellite data collected at McMurdo Station (77°51′S, 166°40′E; Van Woert et al. 1992) during 1988. The satellite imagery was combined with AWS observations (Keller et al. 1989) to conduct a one-year statistical study of mesoscale cyclones. The satellite survey of mesoscale vortices is also extended over the Ross Sea and Ross Ice Shelf regions. Because the results can be highly sensitive to the planetary-scale circulation pattern, they are primarily intended to represent the selected year, although the seasonal variability may apply to other years. This study provides an additional year to the two-year study of mesoscale cyclogenesis conducted by Bromwich (1991) over the southwestern corner of the Ross Sea and near Byrd Glacier, and comparison among these three years allows us to infer some aspects of the interannual variability of mesoscale cyclonic activity. Results of the present study along with a comparative analysis with the results obtained by Bromwich (1991) are presented in the next section. The synoptic-scale pattern associated with mesoscale cyclogenesis is investigated by using the digital Southern Hemisphere analyses constructed by the Australian Bureau of Meteorology (Guymer 1986) for 1988 and for the two years (1984–85) studied by Bromwich (1991). This leads to an evaluation of how the interannual variability of the synoptic-scale pattern can affect the frequency of mesoscale formation. Results of this are included in section 3. Finally, section 4 presents a summary and discussion of this work. For detailed studies of mesoscale cyclogenesis that illustrate the mechanisms involved in the formation and subsequent development of mesoscale cyclones near Terra Nova Bay, the reader is referred to Bromwich (1989b) and Carrasco and Bromwich (1993a).

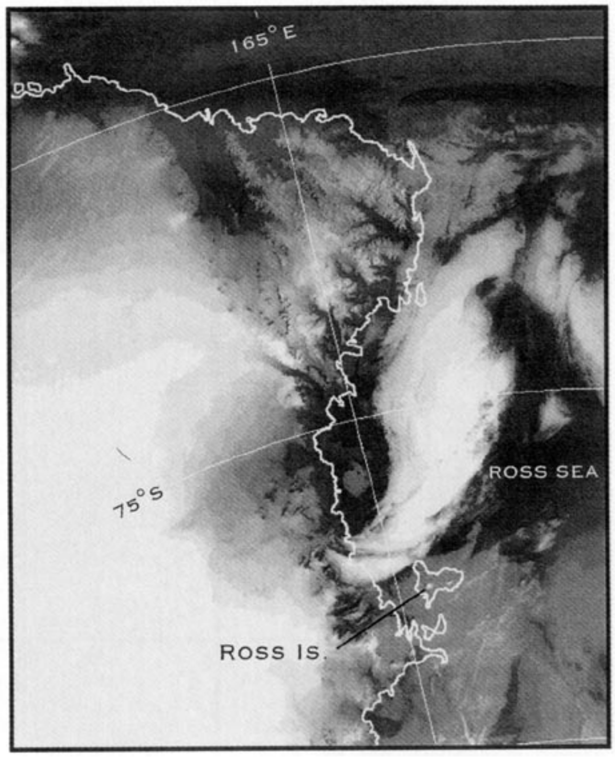


FIG. 3. *NOAA-9* AVHRR thermal infrared satellite image (channel 5) at 0551 UTC 11 February 1988 showing a well-developed deep mesoscale comma-cloud vortex over the southwestern corner of the Ross Sea.

## 2. Mesoscale annual analysis

### a. Satellite analysis results

The present section summarizes a one-year study of mesoscale cyclogenesis activity over the Ross Sea and Ross Ice Shelf areas based on satellite images and regional AWS analyses. The identification of mesoscale cyclones was based upon the cyclonic appearance of the cloud signatures, following the general techniques described in the literature dealing with satellite studies of mesoscale cyclones (e.g., Rasmussen 1981; Lyons 1983; Forbes and Lottes 1985; Businger and Reed 1989; Carleton and Carpenter 1989; Heinemann 1990). Figures 3–6 show examples of mesoscale vortices that illustrate the pattern recognition used in this work. The satellite images were processed in a digital infrared format (AVHRR channel 5: 11.50–12.50 $\mu$m) with a spatial resolution of 3.3 km centered over the southern Ross Sea. This provides a reasonably high resolution image that covers large areas surrounding the Ross Sea and Ross Ice Shelf and allows identification of mesoscale vortices away from the areas near Terra Nova Bay and Byrd Glacier. Also, it permits tracking of the mesoscale cyclones. The capabilities of zooming and/or enhancing (i.e., linear enhancement) the satellite images displayed on the computer screen facilitate identification of mesoscale cyclones. Column 1 in Table 1 gives the number of days per month for which the satellite images were not available. September and October have the largest data gaps. Apart from these months the satellite information was available on average for 24 days per month. All mesoscale cyclones observed through the examination of satellite images were counted and plotted on charts each month. Cyclones observed on more than one image were tracked to determine their trajectories; however, they were counted only once and plotted at the location where they were observed for the first time (initial appearance). Figures 7a–d show the spatial distribution of initial mesoscale cyclone appearance observed for January–February, March–May, June–August, and November–December. These periods represent the distribution for late summer, autumn, winter, and early summer, respectively. This division is based upon the available satellite data, and for subsequent comparison with the integrated satellite imagery and regional AWS analyses. September and October were not included in this satellite analysis due to the lack of images. These months represent the transition period between winter and early summer in the South Polar region. It can be noted that for all periods, points are clustered around Franklin Island and near Byrd Glacier. Many mesoscale vortices were observed over the Ross Sea and Ross Ice Shelf but few of them over the Antarctic plateau.

Columns 2 and 4 in Table 1 specify the number of mesoscale vortices per month observed in the areas defined by Bromwich (1991) (75°–78.5°S and 160°–170°E near Terra Nova Bay/Franklin Island, and

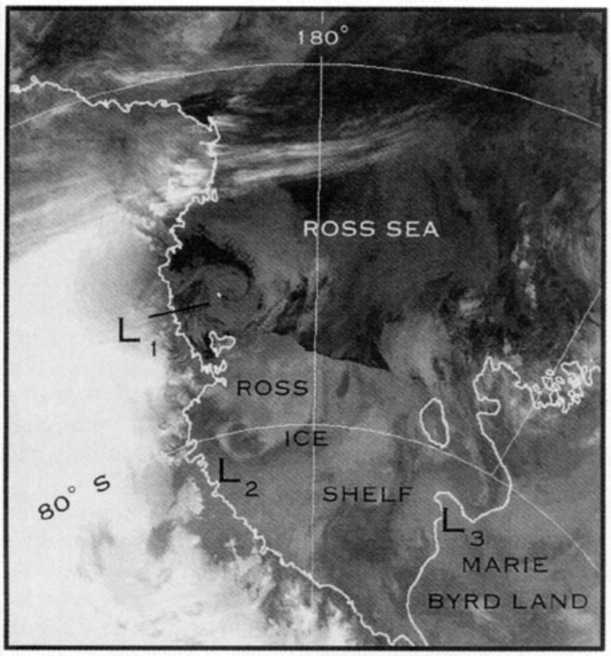


FIG. 4. *NOAA-9* AVHRR thermal infrared satellite image (channel 5) at 1300 UTC 17 February 1988 that shows a very distinctive shallow comma-cloud vortex ($L_1$) over the southwestern Ross Sea, and another much weaker shallow comma-cloud feature ($L_2$) near Byrd Glacier. [For detailed study of the formation and development of these systems see Carrasco and Bromwich (1993a).] Also, a third shallow comma-cloud vortex ($L_3$) can be observed near Marie Byrd Land.

78.5°–82°S and 160°–170°E near Byrd Glacier in Fig. 2), and columns 3 and 5 indicate the normalized weekly frequency for the four periods defined above. The normalized frequency was calculated by dividing the number of mesovortices observed for the given period by one-seventh of the analyzable days. Analyzable days are those days for which at least one satellite image was available. The above calculation yields an unbiased weekly average (normalized weekly frequency) of mesoscale cyclones obtained from examination of satellite images. Thus, around Franklin Island, the largest number of mesoscale vortices was found during both summer periods. On average, 1.9 mesoscale cyclones were observed each week during the early summer, and 2.8 during late summer. The frequency decreases toward the winter, when 1.3 mesoscale vortices on average were observed each week. Near Byrd Glacier, the satellite analysis reveals that the presence of two cyclones each week was found during late summer, but the weekly frequency dropped to one for all the other periods. According to the satellite analyses, around 41% of the Byrd Glacier mesoscale cyclones formed simultaneously with one around Franklin Island (column 6 in Table 1) during 1988.

To study the trajectories of mesoscale cyclones over the Ross Sea and Ross Ice Shelf for the above four periods, all mesoscale vortices were tracked, whenever possible, from the first to last consecutive images upon which they were observable. Figures 8a–d show the mesoscale cyclone tracks for late summer, autumn, winter, and early summer, respectively. It can be seen that, in general, trajectories suggest three sources for mesoscale formation. One is over Marie Byrd Land from whence mesoscale cyclones travel toward the northwest onto the Ross Ice Shelf. Another is suggested near Byrd Glacier; few mesoscale cyclones tracked away from this region even though a large number of vortices formed in this area (Figs. 7a–d). The other area suggested by the trajectories is the southwestern corner of the Ross Sea. Here, the results indicate that, in general, mesoscale cyclones move toward the northeast, and few of them toward the southeast. The satellite imagery analysis of mesoscale cyclone tracks suggests that the cloud signatures associated with them dissipate over the Ross Sea close to their genesis area and/or initial point of satellite detection.

Because a distinctive cloud signature is required for identification of mesoscale cyclones on satellite images, the high frequency observed during the summer period can be related with the sea-ice-free (SIF) (open water) area in the Ross Sea. Figures 7a, 7b, and 7d include the northern edge of the SIF area for selected days according to the Antarctic ice charts prepared by

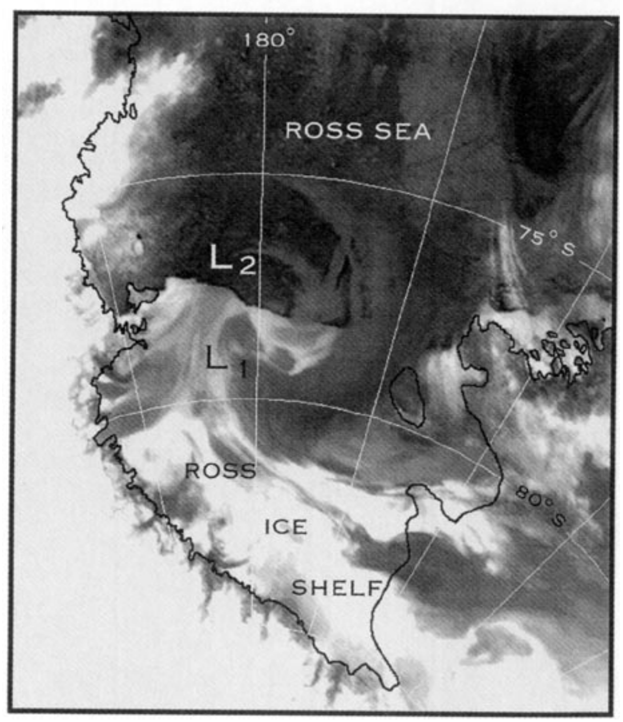


FIG. 5. *NOAA-10* AVHRR thermal infrared satellite image (channel 5) at 1641 UTC 15 July 1988 showing a comma-cloud system ($L_1$) over the Ross Ice Shelf, which is closely followed by another much smaller mesoscale comma vortex ($L_2$).

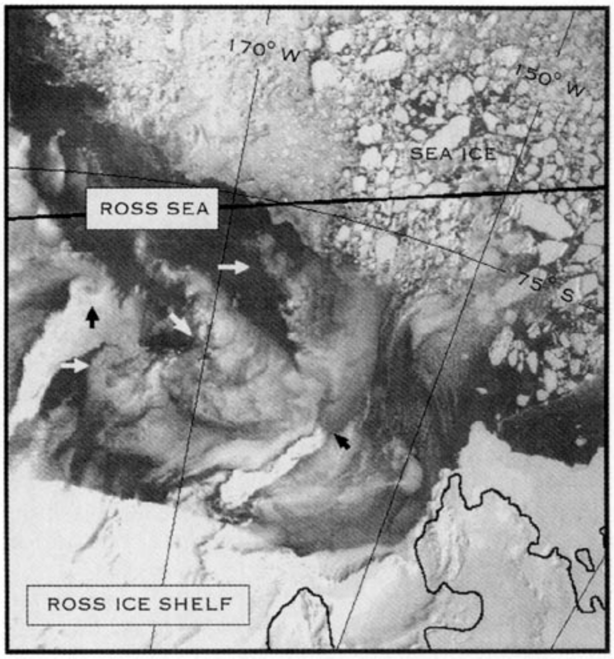


FIG. 6. *NOAA-9* AVHRR visible satellite image (channel 1) at 0338 UTC 8 January 1988 that shows a merry-go-round system (a ring of small vortices, see bold arrows) over the Ross Sea.

the Naval Polar Oceanography Center (1989). During the winter season (Fig. 7c) no SIF area was present in the Ross Sea region. It can be noted that the defined area near Terra Nova Bay/Franklin Island was free of sea ice during late summer, but that the sea ice rapidly built up during early March and then completely covered the area until late December 1988 (Naval Polar Oceanography Center 1989). As Bromwich (1991) noted, this suggests that the role of the open water is to provide the moisture for the distinctive cloud features associated with mesoscale cyclones. This implies that more free-cloud mesoscale cyclones may form during winter. The lower frequency observed near Byrd Glacier in comparison to Terra Nova Bay may be also attributed to the lack of moisture over the ice shelf and to the much colder environment over the Ross Ice Shelf. This may inhibit the formation of a strong boundary layer baroclinic zone associated with katabatic winds coming down through Byrd, Mulock, and Skelton Glaciers.

For late summer (Fig. 8a), the northern half of the Ross Ice Shelf appears to be a dissipation area, as does the northern side of Marie Byrd Land. Over the Ross Sea, some mesoscale vortices dissipated in the area located to the north of Saunders Coast. Figure 7a indicates that during this period a high concentration of sea ice remained over this area. A lack of moisture may inhibit cloud formation associated with the mesoscale cyclones impeding their subsequent identification. Also, because of the presence of sea ice in this area, baroclinic perturbations may weaken when they reach this area due to the colder environment induced by the sea ice making the lower atmosphere more stable than it is over the open ocean.

TABLE 1. Mesoscale cyclogenesis over the southwestern Ross Sea and northwestern Ross Ice Shelf according to purely satellite imagery evaluation during 1988.

| | | Terra Nova Bay/Franklin Island | | Byrd Glacier | | Simultaneous cyclogenesis | |
|---|---|---|---|---|---|---|---|
| Months | Missing days (1) | No. of mesocyclones (2) | Normalized frequency (per 7 days) (3) | No. of mesocyclones (4) | Normalized frequency (per 7 days) (5) | No. of mesocyclones (6) | Percentage |
| January | 6 | 10 | 2.8 | 6 | 2.0 | 2 | 42 |
| February | 11 | 7 | | 6 | | 3 | |
| March | 11 | 5 | 1.7 | 4 | 1.0 | 2 | 30 |
| April | 5 | 5 | | 3 | | 0 | |
| May | 5 | 7 | | 3 | | 1 | |
| June | 4 | 8 | 1.3 | 6 | 0.8 | 3 | 33 |
| July | 4 | 3 | | 3 | | 0 | |
| August | 6 | 3 | | 0 | | 0 | |
| September | 17 | — | — | — | — | — | — |
| October | 25 | — | | — | | — | |
| November | 4 | 8 | 1.9 | 4 | 1.1 | 2 | 53 |
| December | 8 | 5 | | 4 | | 3 | |
| Total | 106 | 61 | | 39 | | 16 | 41 |
| Weekly average | | 2 | 1.8* | | 1.1* | | |

* Not including September and October.

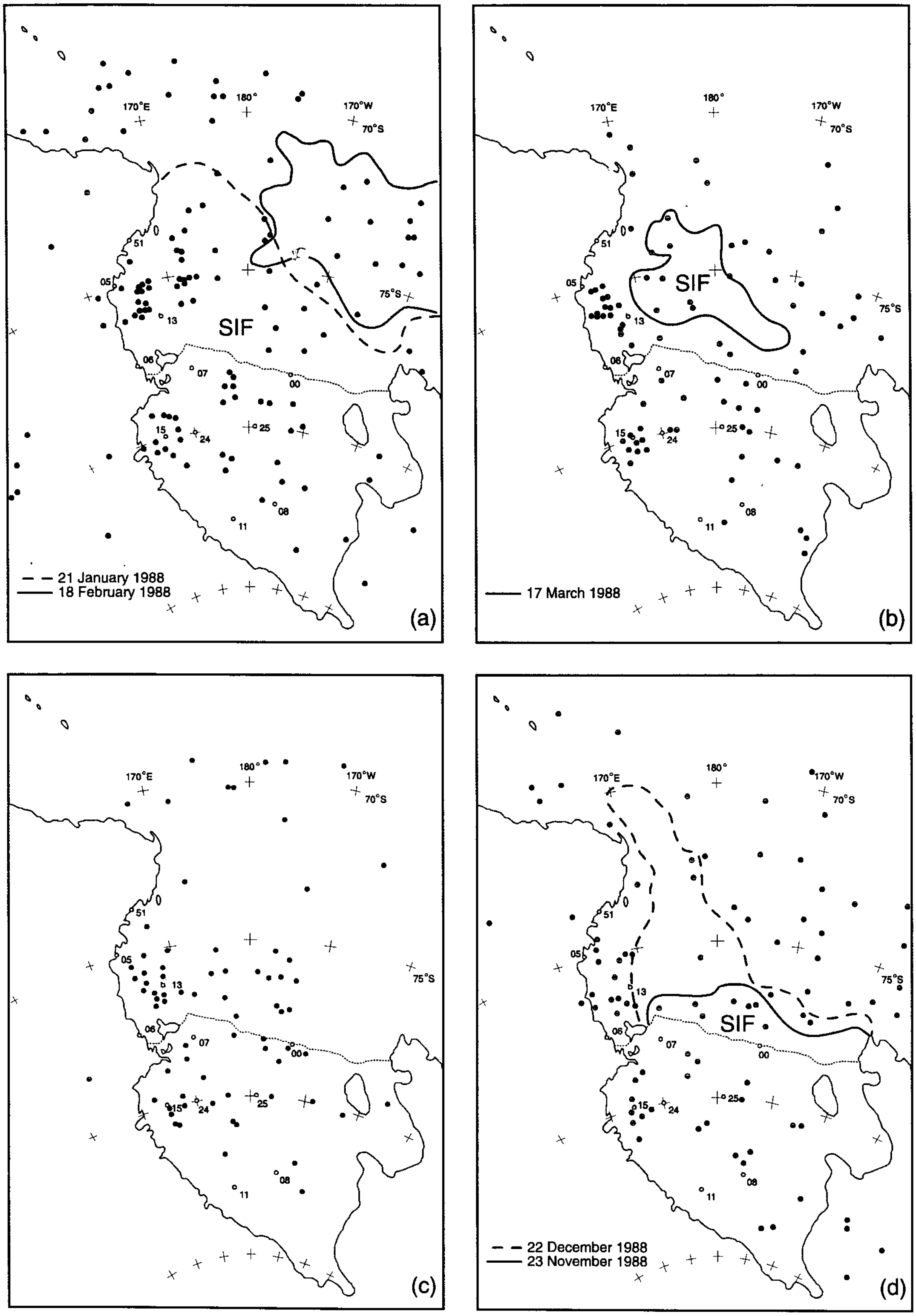


FIG. 7. Seasonal spatial distribution of the mesoscale vortices observed on satellite images (small dots) for (a) late summer, (b) autumn, (c) winter, and (d) early summer. Numbers attached to open circles identify AWS sites. SIF denotes sea-ice-free area where dashed and solid lines indicate locations of the northern limits of the sea ice. For 23 November, the solid line encloses sea-ice concentrations of 0.1–0.3.

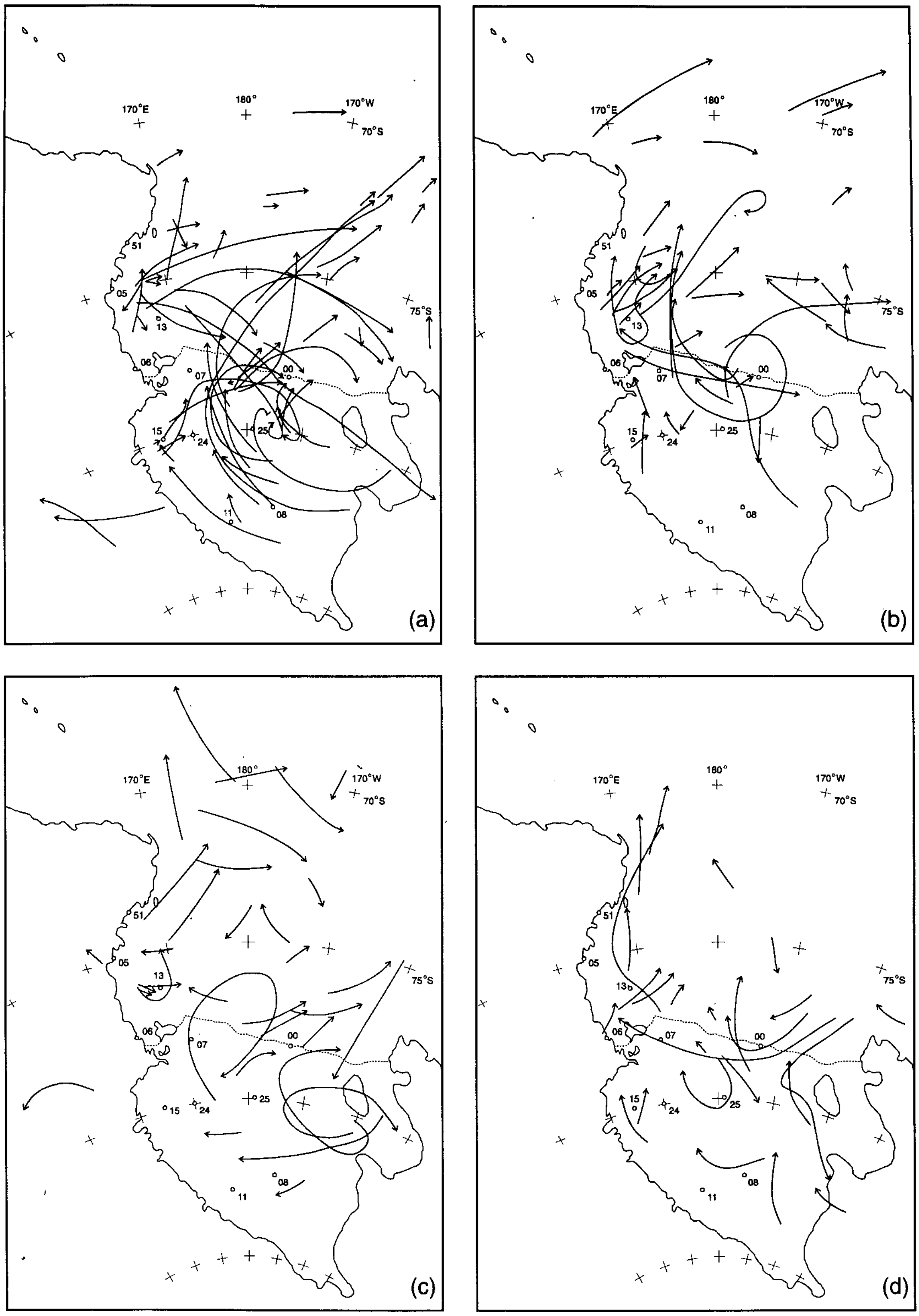


FIG. 8. Trajectories of mesoscale cyclones observed on satellite images for (a) late summer, (b) autumn, (c) winter, and (d) early summer.

TABLE 2. Annual summary of the satellite classification of mesoscale vortices observed near Terra Nova Bay and Byrd Glacier within the areas defined in Fig. 2 (Bromwich 1991). Also, results over the Ross Sea and Ross Ice Shelf (outside of the defined areas) are listed; No.—number of mesoscale vortices, *d*—diameter in kilometers, *P*—percentage of mesovortices with respect to the total number. Bold numbers indicate percentage of deep vortices, and bold/underlined numbers indicate normalized annual weekly frequency, respectively.

| | No. | *d* (km) | *P* | | No. | *d* (km) | *P* | |
|---|---|---|---|---|---|---|---|---|
| | Near Terra Nova Bay | | | | Near Byrd Glacier | | | |
| Comma cloud | 48 | 179 | 78.7% | | 29 | 175 | 74.3% | |
| Spiraliform | 6 | 189 | 9.8% | | 8 | 195 | 20.5% | |
| Merry-go-round | 4 | 325 | 6.6% | | 1 | 336 | 2.6% | |
| Oval, solid mass | 1 | 321 | 1.6% | | | | | |
| Single shallow band | 2 | 77 | 3.3% | | 1 | 134 | 2.6% | |
| Total vortices | 61 | 190 | **9.8%** | **<u>1.8</u>** | 39 | 184 | **10.3%** | **<u>1.1</u>** |
| | Over Ross Sea region | | | | Over Ross Ice Shelf region | | | |
| Comma cloud | 138 | 256 | 67.6% | | 82 | 293 | 78.9% | |
| Spiraliform | 32 | 339 | 15.5% | | 12 | 307 | 11.5% | |
| Merry-go-round | 28 | 327 | 13.5% | | 4 | 351 | 3.8% | |
| Oval, solid mass | 5 | 367 | 2.4% | | 5 | 276 | 4.8% | |
| Multiple shallow bands | 1 | 264 | | | 1 | 210 | 1% | |
| Swirl in cumulus streets | 2 | 149 | 2.0% | | | | | |
| Single shallow band | 1 | 72 | | | | | | |
| Total vortices | 207 | 282 | **18.4%** | **<u>6.0</u>** | 104 | 294 | **20.2%** | **<u>3.0</u>** |

The satellite-observed mesoscale vortices near Terra Nova Bay and Byrd Glacier [within the areas defined by Bromwich (1991) (Fig. 2)] were classified according to the initial cyclonic shape of the cloud signatures associated with them. A similar analysis was carried out for all the mesovortices observed over the Ross Sea and Ross Ice Shelf regions but outside of the areas defined near Terra Nova Bay and Byrd Glacier. The categorization of the cloud patterns followed Forbes and Lottes (1985), although no subdivision was made for comma-cloud types, and the spiraliform types were counted separately from the comma ones. Also, the diameter of all the vortices identified on satellite images was measured. This was given by the distance from edge to edge of the cyclonic signature apparently associated with them. Spiraliform clouds are almost symmetric and their diameters are easily measured once the vortical cloud is defined. Comma-cloud vortices have a frontlike shape; their diameter was measured from the rear edge to the front edge of the head of the vortical cloud. Merry-go-round features are systems of two or more very small vortices (Fig. 6); their diameters were given by the longer distance from edge to edge that includes all the vortical clouds. No minimum diameter was required. In addition, the depth of the vortical cloud was estimated in a qualitative fashion because radiosonde data were not available for this research. Thus, to obtain the vertical extent of vortices, the brightness of the cloud signature associated with them on infrared satellite images was noted. Low (middle and high) cloud in infrared satellite images appears as dark or gray (white or light) tones; therefore, dark or gray vortical cloud identifies shallow vortices, and white cloud signatures identify deep vortices. However, a limited random survey of the cloud-top temperatures (CTT) associated with the mesoscale vortices observed over the Ross Sea and Ross Ice Shelf region (including the defined areas in Fig. 2) was conducted to obtain a quantitative estimate of the cloud-top height associated with vortices. The seasonal average CTT were compared with climatological temperature profiles (11-year average, 1972–82) at McMurdo Station. For this, it is assumed that most of the clouds (except cirrus) are nearly blackbodies, implying that their emissivity is close to 1. Therefore, average retrieved CTT for each season corresponds closely to the seasonal average of the physical temperatures as measured by the radiosonde. CTT for dark clouds range from $-16.2° \pm 5.1°$ to $-28.4° \pm 3.3°C$ (1 sd; $n = 30$ and $n = 39$) from summer to winter. These temperatures correspond to heights of 2100 and 2300 m, respectively, which are below 700 hPa. For white clouds, the CTT range from $-27.8° \pm 2.1°$ to $-45.9° \pm 5.1°C$ (1 sd; $n = 16$ and $n = 14$) from summer to winter. The climatological sounding data position these values at 4400-m ($\approx$580 hPa) and 6300-m ($\approx$450 hPa) height, respectively. It must be mentioned that the cloud-top heights as derived from the CTT must be viewed with caution; they may not necessarily correspond to the depth of the vortices, and the CTT values were compared with climatological temperature profiles and not with simultaneous soundings, due to the unavailability of these data for 1988.

Table 2 summarizes the findings for the entire year; because of the shortage of images in September and

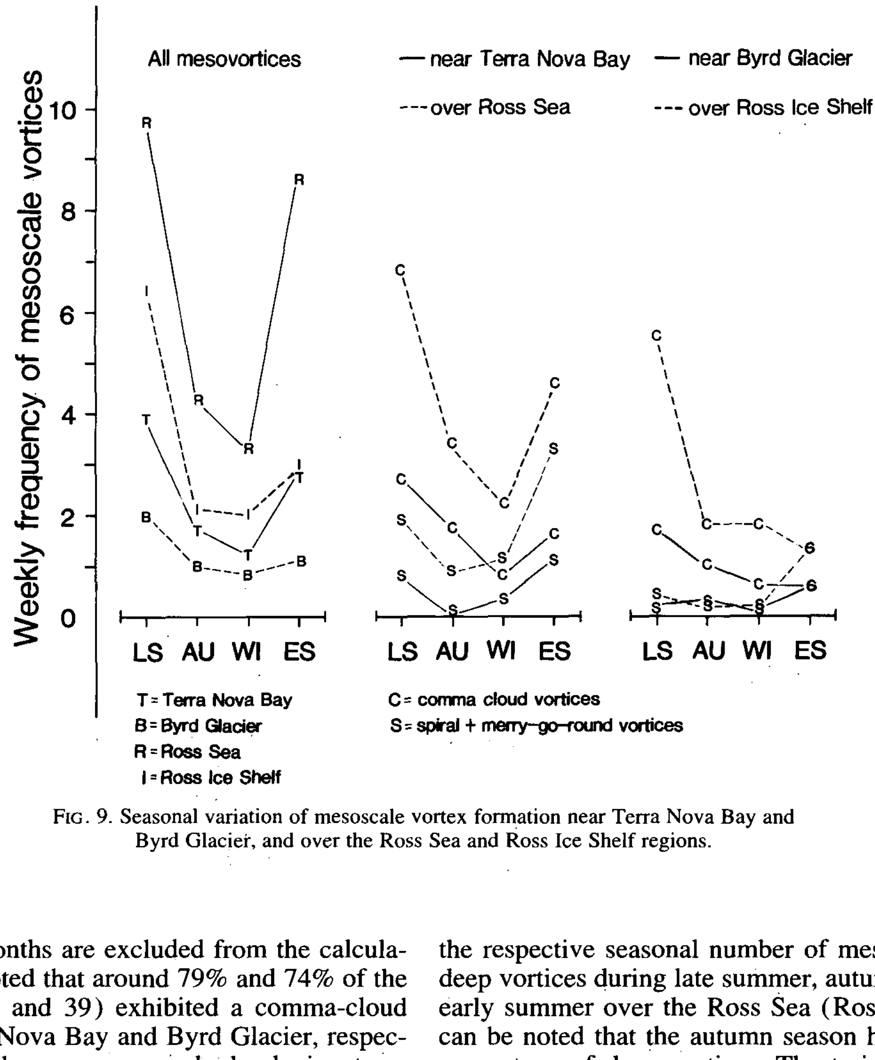


FIG. 9. Seasonal variation of mesoscale vortex formation near Terra Nova Bay and Byrd Glacier, and over the Ross Sea and Ross Ice Shelf regions.

October, these months are excluded from the calculations. It can be noted that around 79% and 74% of the total vortices (61 and 39) exhibited a comma-cloud shape near Terra Nova Bay and Byrd Glacier, respectively. Spiral and merry-go-round cloud signatures were the second and third most frequent types observed at both locations. The average diameter for all the vortices was about 190 and 184 km near Terra Nova Bay and Byrd Glacier, respectively. On average, comma types have the smallest diameter (179 and 175 km, respectively). Only around 10% (6 out of 61 and 4 out of 39) of the vortices showed middle/high cloud associated with them, suggesting that the vast majority of the mesovortices are shallow—that is, a vertical extent below 700 hPa according to the CTT analysis. Four (three) of the deep vortices occurred during the late summer near Terra Nova Bay (Byrd Glacier), and none was observed during the autumn in either area.

In general, the same results were found over the extended regions of the Ross Sea and Ross Ice Shelf. The respective average diameters of all the vortices in these regions were 282 and 294 km, which are larger than those measured near Terra Nova Bay and Byrd Glacier. Also the percentage of deep vortices were 18% (38 out of 207) and 20% (21 out of 104), respectively. Around 23%, 5%, 24%, and 18% (33%, 0%, 4%, and 35%) of the respective seasonal number of mesovortices were deep vortices during late summer, autumn, winter, and early summer over the Ross Sea (Ross Ice Shelf). It can be noted that the autumn season has the smallest percentage of deep vortices. The trajectories suggest that some of the vortices over the Ross Sea and Ross Ice Shelf could have formed near Terra Nova Bay and Byrd Glacier, and some of them over southern Marie Byrd Land. This may indicate that on average the vortices observed over the Ross Sea and Ross Ice Shelf regions are more mature in comparison with those observed near Terra Nova Bay and Byrd Glacier. Also, mesovortices over the Ross Sea and Ross Ice Shelf may be the remnants of synoptic-scale cyclones that decay near and/or over Marie Byrd Land. The annual numbers of mesovortices observed per unit area ($10^4$ $km^2$) are 6.1 near Terra Nova Bay, 5.2 near Byrd Glacier, 2.5 over the Ross Sea, and 1.8 over the Ross Ice Shelf. In other words, while 61 (39) mesovortices were observed during 1988 within the defined area near Terra Nova Bay/Franklin Island (near Byrd Glacier), 25.2 (13.5) mesovortices per equivalent area were detected over the rest of the Ross Sea (Ross Ice Shelf). This indicates that much higher activity occurs near Terra Nova Bay and Byrd Glacier than outside of these two areas. Figure 9 shows the normalized weekly frequency of all the vortices near Terra Nova Bay and Byrd Glacier as well as over the Ross Sea and Ross Ice Shelf regions. The normalized weekly frequency of comma and spiral/merry-go-round vortices are also shown in Fig. 9. As mentioned above, the maximum number of vortices was found during late and early summers. The three dominant types of vortices exhibit the same behavior over the Ross Sea as they do near Terra Nova Bay. On the other hand, results indicate that the number of comma shapes that dominate during the late summer near Byrd Glacier and over the Ross Ice Shelf decreases through the year, while the number of spiral and merry-go-round vortices increases. Overall, from this survey, mesoscale cyclonic activity over the entire study area (Figs. 7a–d) was quite frequent. On average seven to eight and three to four mesoscale vortices were observed each week over the Ross Sea and Ross Ice Shelf (including the areas near Terra Nova Bay and Byrd Glacier), respectively, with comma clouds being the dominant type of vortices observed.

Previously, Carleton and Carpenter (1989) through the examination of seven years (1977–83) of hard-copy DMSP satellite imagery of 5.4-km resolution for the winter months (June–September) had already found that the comma-cloud vortices dominate (91% of the total vortices) over the Southern Hemisphere. Later, Carleton and Fitch (1993) carried out a similar mesoscale cyclone classification but for the winter months (June–August) of 1988 and 1989. Carleton and Fitch (1993) used the same kind of hard-copy DMSP imagery, which was merged into mosaics that covered half of the hemisphere south of 50°S, and from 120°E to 60°W. Few mesoscale cyclones were found over the Ross Sea and Ross Ice Shelf regions, which does not agree with the number of vortices found in this study. This is probably due to the different format and resolution of the satellite imagery; the availability of digital imagery for our investigation is the primary reason for our better identification of the vortices. As they recognized, their results are probably most representative of the area between 50° and 70°S. The present study covered the Ross Sea and Ross Ice Shelf, and results are most representative of the area south of 70°S and between 160°E and 160°W (see Figs. 7a–d). Therefore, both studies, at least during the winter, complement each other. The normalized monthly number of mesovortices observed by Carleton and Fitch (1993) in their entire area for the three winter months was 204 vortices; in our case, it was 96 vortices. If these numbers complement each other, this reveals a very large mesoscale cyclonic activity over the Ross Sea–Ross Ice Shelf region, at least in 1988. Carleton and Fitch's (1993) results also indicate the dominance of comma-cloud vortices over their study region. In particular, for the winter of 1988, they obtained 52% in June, 61% in July, and 38% in August. The results from this study over the Ross Sea (including the Terra Nova Bay area) are 76% in June, 82% in July, and 44% in August, indicating similar behavior.

### *b. Integrated satellite and regional AWS analyses*

Integration of the mesoscale sea level analyses with the satellite images provides a more complete monthly overview of the mesoscale cyclogenesis around Franklin Island and near Byrd Glacier. Pressure analyses were constructed twice a day (0000 and 1200 UTC) for the entire year using the AWS data (Keller et al. 1989). The results of the integrated analysis for 1988 are given in Table 3. Columns 1 and 2 include all vortices that could be analyzed on at least one chart, and those revealed by the satellite images, but because of their size they were not resolved by the sea level pressure fields. A monthly average of 10.2 (about 2 each week) mesoscale cyclones formed over the southwestern corner of the Ross Sea, while 5.3 (almost 1 each week) were resolved near Byrd Glacier. A weak monthly frequency maximum was found for January and February (late summer) in both areas. The percentage of mesoscale cyclones formed at Byrd Glacier simultaneously with those near Franklin Island (±12 h) was, on average, about 78% overall. Note that this percentage increased with respect to the percentage given by the satellite imagery analysis alone. This is probably because the sea level pressure field resolved mesoscale cyclones near Terra Nova Bay that do not have a distinctive cloud signature associated with them. Columns 4 and 5 in Table 3 give the percentage of significant mesoscale cyclones that formed near Franklin Island and Byrd Glacier, respectively. A cyclone was generally considered to be significant if the wind speed recorded at Franklin Island (AWS 13) was at least 7.5 m $s^{-1}$ and two isobars, analyzed every 2 hPa, encircled the center. Cyclones that were encircled by one isobar but had another isobar suggesting a deep trough were also considered significant. The same criterion was applied for the area near Byrd Glacier but using AWS 15 and/or 24 (Bromwich 1991). Because AWS 15 site failed at the end of July, data are not available from August onward; therefore, results near Byrd Glacier are somewhat uncertain. A monthly average of 23% and 16% of the cyclones were counted as significant around Franklin Island and near Byrd Glacier, respectively. In fact, no significant cyclones were analyzed in either area during the last quarter of the year (early summer).

Columns 6 and 8 in Table 3 show the average duration of the mesoscale cyclones near Terra Nova Bay/Franklin Island and Byrd Glacier, respectively. This was estimated from the first time that a cyclone was analyzed within the domain (Fig. 2) until it disappeared from the analysis or moved away from the domain according to the sea level pressure analyses. About 39% (56%) of the cyclones were found on just one chart near Terra Nova Bay (Byrd Glacier). These

TABLE 3. Mesoscale cyclogenesis over the southwestern Ross Sea (near Terra Nova Bay/Franklin Island) and northwestern Ross Ice Shelf (near Byrd Glacier) according to the integrated analysis of satellite imagery and regional sea level pressure charts. Numbers in square brackets indicate weekly average.

| Month | Number of cyclones formed: Near Franklin Island (1) | Number of cyclones formed: Near Byrd Glacier (2) | Percent of Byrd's cyclones forming simultaneously with those at Franklin Island (±12 h) (3) | Percent of significant cyclones: Near Franklin Island (4) | Percent of significant cyclones: Near Byrd Glacier (5) | Average duration of cyclones formed near Franklin Island (12 h) (6) | Maximum intensity of cyclones formed near Franklin Island (hPa) (7) | Average duration of cyclones formed near Byrd Glacier (12 h) (8) | Maximum intensity of cyclones formed near Byrd Glacier (hPa) (9) |
|---|---|---|---|---|---|---|---|---|---|
| January | 14 | 10 | 80 | 7 | 0 | 2.1 | 2.4 | 1.8 | 1.1 |
| February | 12 | 7 | 100 | 17 | 14 | 2.9 | 3.5 | 2.7 | 1.7 |
| March | 9 | 6 | 83 | 33 | 17 | 2.9 | 3.2 | 1.7 | 1.8 |
| April | 13 | 4 | 75 | 39 | 50 | 2.2 | 2.8 | 1.8 | 2.0 |
| May | 12 | 3 | 100 | 33 | 33 | 2.2 | 2.8 | 1.3 | 2.0 |
| June | 9 | 6 | 83 | 22 | 17 | 2.0 | 1.6 | 1.2 | 1.2 |
| July | 11 | 6 | 67 | 36 | 50 | 2.4 | 3.1 | 1.2 | 2.2 |
| August | 9 | 5 | 60 | 22 | 20 | 1.8 | 3.4 | 1.2 | 1.2 |
| September | 9 | 5 | 60 | 33 | 0 | 1.8 | 2.8 | 1.0 | 1.6 |
| October | 7 | 1 | 100 | 0 | 0 | 1.6 | 3.0 | 1.0 | 1.0 |
| November | 8 | 6 | 50 | 0 | 0 | 1.5 | 2.0 | 1.8 | 1.2 |
| December | 9 | 5 | 80 | 0 | 0 | 1.6 | 2.0 | 1.6 | 1.2 |
| Monthly average | 10.2 [2.4] | 5.3 [1.3] | 78 | 23 | 16 | 2.1 | 2.7 | 1.5 | 1.5 |

cyclones are assumed to have a duration of about 12 h (Bromwich 1991). Figure 10a shows the distribution of cyclone durations (in units of 12 h) for the present study and those for 1984 and 1985 obtained by Bromwich (1991) that occurred near Terra Nova Bay. Almost 33% of the cyclones in 1988 lasted about 24 h, and about 72% had a duration of one day or less. In addition, about 12% lasted around 36 h. About 16% of the total cyclones had a duration over 36 h, but only three of them lasted more than three days. The monthly average was around 25 h (2.1 × 12 h) with February and March being the months that had the longest durations (about 35 h), while November had the shortest (about 18 h). Near Byrd Glacier the monthly average was around 18 h (1.5 × 12 h) with a maximum during February and minimum in September and October. Columns 7 and 9 in Table 3 indicate the maximum intensity of the mesoscale vortices near Terra Nova Bay/Franklin Island and Byrd Glacier, respectively. The intensity was estimated as the pressure difference between the periphery of each cyclone and its center. The results do not reveal a seasonal variation of the maximum cyclone intensity. About 42% of the cyclones had an intensity of 2 hPa (Fig. 10b), and the monthly average maximum intensity was about 2.7 hPa near Terra Nova Bay/Franklin Island; around 92% of the mesoscale cyclones near Byrd Glacier had an intensity equal to or less than 2 hPa. This reveals that the mesoscale cyclones in this area are generally weaker than those near Terra Nova Bay.

Columns 1 and 2 (3 and 4) in Table 4 indicate the weekly average of mesoscale cyclones near Terra Nova Bay/Franklin Island (Byrd Glacier) for each period according to the purely satellite evaluation and to the integrated analysis of satellite imagery and regional sea level pressure charts. This shows that over the southwestern corner of the Ross Sea the integrated analyses give a slightly higher frequency of mesoscale cyclones than that obtained through the examination of satellite images alone. This difference becomes more marked in winter when about 45% of the vortices were missing from the satellite images. This suggests that the lack of moisture due to the sea ice prevents almost half of the mesoscale cyclones near Terra Nova Bay/Franklin Island from developing a distinctive cloud signature that can be associated with the vortex. On the other hand, results indicate that practically all the mesovortices observed during autumn and late and early summers near Byrd Glacier were resolved by the AWS analyses. However, the percentage of mesoscale cyclones introduced by the integrated analyses increases during the winter, where about 38% of them did not develop a distinctive cloud signature. This may be due to the location of Byrd Glacier, far to the south of the northern edge of the Ross Ice Shelf, so that the influence of the seasonal variation of the sea ice is less marked. That is, the lack of moisture near Byrd Glacier does not vary significantly throughout the year. The above results in-

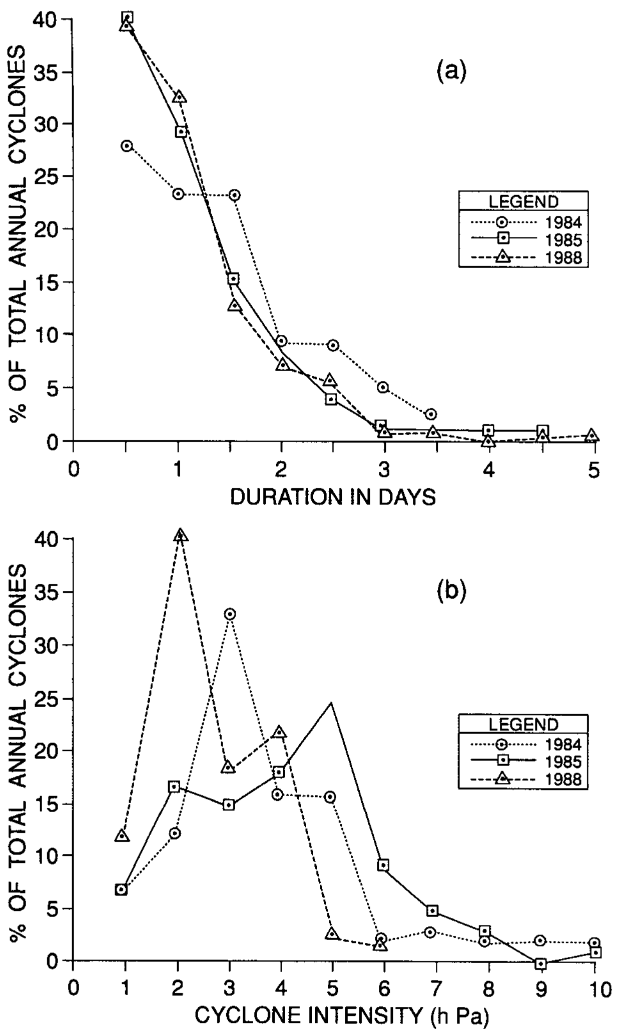


FIG. 10. Frequency distribution of (a) mesoscale cyclone duration and (b) maximum intensity near Franklin Island. Data for 1984 and 1985 are from Bromwich (1991).

dicate that it mostly takes warm and moist air advection to yield cyclogenesis near Byrd Glacier, whereas outbreaks of cold katabatic air over the southwestern corner of the Ross Sea can form mesoscale cyclones without warm and moist air advection, implying more cloud-free mesoscale cyclones forming in this area. In addition, a greater thermal contrast can form near Terra Nova Bay, which is more likely to be affected by passing synoptic-scale cyclones advecting warm air and enhancing the semipermanent subsynoptic surface trough over the western Ross Sea.

In general, the larger mesoscale cyclonic activity over the Ross Sea compared to the Ross Ice Shelf can be related to more frequent warm-air advection associated with synoptic-scale cyclones passing through or decaying just to the northeast of the Ross Sea. On the other hand, katabatic airflow coming from East and West Antarctica can cross the entire Ross Ice Shelf and reach the Ross Sea. The merging of advected warm air and cold katabatic air can create zones of strong thermal contrast that support mesoscale cyclogenesis. These zones may not form as frequently over the Ross Ice Shelf as over the Ross Sea. Also, the relatively larger in situ surface heating over the Ross Sea can contribute to the larger mesoscale cyclonic activity in this area.

### *c. Synoptic-scale circulation accompanying mesoscale cyclogenesis during 1988*

To study the synoptic-scale environment accompanying mesoscale cyclogenesis at Terra Nova Bay/Franklin Island, averages were calculated for all the cyclogenesis events at the time when the cyclones were resolved for the first time by the integrated regional AWS analyses and satellite imagery evaluation (122 events). The Australian digital Southern Hemispheric data [500-km horizontal resolution (Guymer 1986)] that provide analyses for sea level pressure (or 1000 hPa), 500 hPa, and the 1000–500-hPa geopotential thickness were used. The synoptic-scale average for all cyclogenesis events (CEA hereafter) was compared with the annual average to examine changes in the large-scale circulation. The sea level pressure annual average and the differences between the averages (where stippled areas are significantly different at better than the 95% confidence level using a two-tailed $t$ test) are shown in Figs. 11a and 11b, respectively. These results are intended to explain only the mesoscale cyclonic activity near Terra Nova Bay/Franklin Island and not the activity over the rest of the Ross Sea and Ross Ice Shelf. In general, both averages showed very similar patterns. The difference between them is slightly amplified over Victoria Land and the northwestern Ross Sea where for cyclogenesis days there is lower pressure. The $t$ test indicates that this decrease of the pressure field is statistically significant. The same results were obtained for the CEA for late summer and winter (not shown), which revealed small changes relative to their respective averages. The 500-hPa and 1000–500-hPa anomaly fields (not reproduced) are similar to those found at sea level pressure. The 500-hPa average height field for the CEA showed significantly (in statistical sense) lower geopotential heights just over northern Victoria Land. However, the changes of the 1000–500-hPa geopotential thickness observed for CEA were not statistically significant.

Some localized minor changes appear around the Antarctic continent to the north of 60°S (Fig. 11b) but they cannot be linked to synoptic features that play a significant and/or direct role in cyclogenesis over the southwestern Ross Sea. The broadscale results suggest that cyclogenesis may be associated with changes in the synoptic-scale pattern that takes place over the western Ross Sea and the area immediately to the north

TABLE 4. Seasonal weekly frequencies of mesoscale cyclones over the southwestern Ross Sea and northwestern Ross Ice Shelf according to purely satellite evaluation (normalized) and to the integrated analyses of satellite imagery and regional sea level pressure charts during 1988.

| | Weekly average | | | | |
|---|---|---|---|---|---|
| | Franklin Island | | Byrd Glacier | | |
| Month | Satellite detection (1) | Satellite + AWS analyses (2) | Satellite detection (3) | Satellite + AWS analyses (4) | Defined season |
| January February | 2.8 | 3.0 | 2.0 | 2.0 | Late summer |
| March April May | 1.7 | 2.6 | 1.0 | 1.0 | Autumn |
| June July August | 1.3 | 2.2 | 0.8 | 1.3 | Winter |
| September October | — | — | — | — | |
| November December | 1.9 | 2.0 | 1.1 | 1.3 | Early summer |
| Annual* | 1.8 | 2.4 | 1.1 | 1.2 | |

* Excluding September and October.

and west of it (Fig. 11). These changes suggest the presence of synoptic-scale cyclones or troughs to the west of the Ross Sea entrance (Bromwich 1991). On the other hand, the lower 500-hPa geopotential heights for cyclogenesis days suggest upper-level troughs just to the northwest of the area of cyclogenesis. The po-

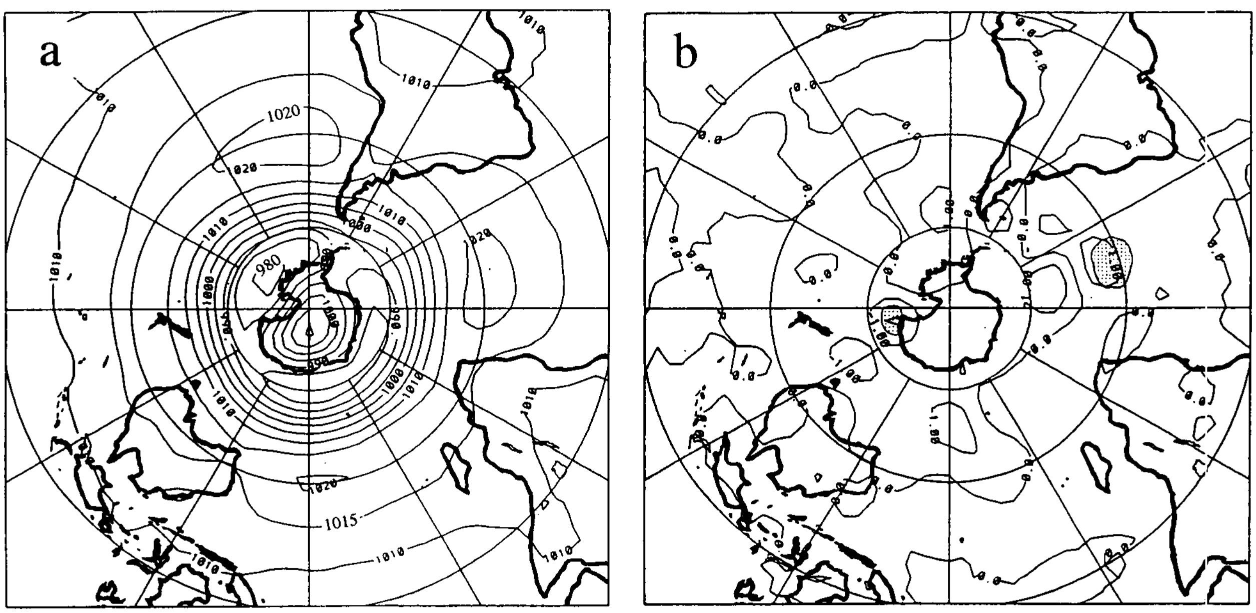


CONTOUR FROM 975 TO 1020 CONTOUR INTERVAL OF 5 hPa

CONTOUR FROM -2.0 TO 1.0 CONTOUR INTERVAL OF 1

FIG. 11. Southern Hemisphere sea level pressure analyses for 1988: (a) annual average and (b) pressure anomalies for the cyclogenesis days with respect to the annual average. Stippled areas are statistically different from zero at better than the 95% confidence level using a two-tail $t$ test.

sition of such a trough can facilitate formation and subsequent development of mesoscale cyclones by advecting cyclonic vorticity over the Ross Sea area.

The surface and 500-hPa synoptic-scale averages and the anomalies with respect to the annual averages (not reproduced) for all significant and/or deep mesoscale cyclones within the defined area near Terra Nova Bay show that these events are associated with a deeper quasi-stationary synoptic surface low and polar vortex at 500 hPa centered over the Ross–Amundsen Sea area. This synoptic pattern supports 1) warm-air advection over the Ross Sea–Ross Ice Shelf area associated with synoptic storms decaying near Marie Byrd Land, and 2) enhanced katabatic air outflow from East Antarctica into the southwestern corner of the Ross Sea. This synoptic pattern resembles that found in association with katabatic air outbreaks over the Ross Sea/Ross Ice Shelf coming from West Antarctica [see Bromwich et al. (1992, 1993a, 1994) for study of katabatic surge events]. Further investigation is needed of these cases and their relation to katabatic surges, which is beyond the scope of this article.

## 3. Interannual comparison between mesoscale cyclogenesis over southern Ross Sea

### a. *Comparison between 1985 and 1988 mesoscale cyclogenesis*

A comparison with the results obtained by Bromwich (1991) for 1985 is included in Table 5. Because mesoscale analyses were not available for January 1984 and no observations were collected in Terra Nova Bay between April and October in 1984, no comparison was conducted with this year because the uncertainty of the pressure analyses (Bromwich 1991). Table 5 shows that overall 1988 had more mesoscale cyclogenesis in both areas (columns 1 and 2 in Table 5), as well as more simultaneous formation, but as for 1985, two mesoscale cyclones on average formed each week near Franklin Island. In particular, in terms of the seasonal breakdown discussed earlier, larger weekly mesoscale cyclogenesis activity was found during the late summer (January–February) and autumn (March–May) seasons for 1988 than for 1985. On the other hand, almost the same weekly activity was resolved for both years throughout the winter, spring, and early summer. The maximum weekly mesoscale cyclogenesis activity that occurred during the winter in 1985 was found during the summer in 1988. This shift took place in both the Terra Nova Bay and Byrd Glacier areas. A weekly minimum occurred during the spring (September–October) at both areas in 1988.

The percentages of mesoscale cyclones exhibiting significant intensification during 1988 are significantly lower than for 1985 (columns 4 and 5 in Table 5). This difference is more marked for spring and late and early summers. Comparing the duration and intensity of the mesoscale cyclones between 1988 and 1985 [columns 6 and 7 in Table 5 (Figs. 10a and 10b)], it can be noted that for 1988 the duration was slightly shorter than 1985 but the maximum intensity was significantly lower than 1985, mainly during the winter and early summer seasons. This indicates that, although mesoscale cyclogenesis was slightly more frequent during 1988, the resulting mesoscale cyclones were weaker and less persistent than those in 1985. On the other hand, in 1984, Bromwich (1991) found that the weekly average of cyclones formed in the Terra Nova Bay–Franklin Island area was less than 1, but the percentage of significant cyclones was similar to 1985. To investigate these interannual variations and their possible relation with year-to-year variations in the large-scale circulation, synoptic-scale annual and CEA averages were constructed for 1984 and 1985.

### b. *Comparison of the synoptic-scale pattern between 1984–85 and 1988*

Figures 12a and 12b are the annual average sea level pressure field and the differences between the CEA and the annual average for 1984, respectively. Figures 13a and 13b are for 1985. As in 1988, comparison between both averages (Fig. 12b) shows that, in general, changes of a few hectopascals (2–3) take place. These were statistically significant over Victoria Land in 1984 but not in 1985 (Fig. 13b). The results indicate that the negative departures of the 500-hPa geopotential heights and the 1000–500-hPa geopotential thickness (not reproduced) are not statistically significant near the area of interest (Ross Sea/Ross Ice Shelf). This confirms the anomalies obtained by Bromwich (1991, Table 4) for individual stations in 1984–85.

In 1984, the largest difference at the surface (in the area of interest) is located over the western Ross Sea and Victoria Land, while at 500 hPa, it is over the plateau and to the north of the Wilkes Land coast. In 1985, no statistically significant changes are observed in the area of interest, while at 500 hPa, the largest difference is found to the north of the Ross Sea, over the South Pacific Ocean. The position of the negative departures indicates a difference between 1984 and 1985. In comparing 1984 and 1985 with 1988, it was noted that the negative departures of the sea level pressure over the western Ross Sea/Victoria Land in 1984 (1985), although larger, are similar (different) to those observed in 1988.

The number of mesoscale cyclones, total and significant, for 1984 differs from 1988, despite these two years seeming to have the same large-scale environment associated with cyclogenesis, in terms of the absolute values of the sea level pressure and 500-hPa height fields. A possible explanation for this could be the fact that for 1984, AWS data from Terra Nova Bay were not available after 19 April 1984. Because of its location this station provides key information for de-

TABLE 5. Comparison of mesoscale cyclogenesis between 1985 (Bromwich 1991) and 1988.

| Month | Weekly average of cyclones formed: Near Terra Nova Bay/Franklin Island (1) | | Weekly average of cyclones formed: Near Byrd Glacier (2) | | Percent of Byrd's cyclones forming simultaneously with those near Terra Nova Bay/Franklin Island (±12 h) (3) | | Percent of cyclones considered to be significant near: (4) Terra Nova Bay/Franklin Island | | Percent of cyclones considered to be significant near: (5) Byrd Glacier | | Average duration (6) Terra Nova Bay/Franklin Island | | Average maximum intensity (7) Terra Nova Bay/Franklin Island | |
|---|---|---|---|---|---|---|---|---|---|---|---|---|---|---|
| | 1985 | 1988 | 1985 | 1988 | 1985 | 1988 | 1985 | 1988 | 1985 | 1988 | 1985 | 1988 | 1985 | 1988 |
| January | 1.5 | 3.2 | 0.7 | 2.3 | 67 | 80 | 0 | 7 | 67 | 0 | 2.9 | 2.1 | 2.1 | 2.4 |
| February | 0.8 | 2.9 | 0.8 | 1.7 | 33 | 100 | 86 | 17 | 33 | 14 | 4.6 | 2.9 | 4.9 | 3.5 |
| | 1.6 | 3.0 | 0.7 | 2.0 | 50 | 90 | 43 | 12 | 50 | 7 | 3.8 | 2.5 | 3.5 | 3.0 |
| March | 1.8 | 2.0 | 0.7 | 1.4 | 67 | 83 | 63 | 33 | 67 | 17 | 2.6 | 2.9 | 3.5 | 3.2 |
| April | 2.1 | 3.0 | 0.5 | 0.9 | 50 | 65 | 11 | 39 | 50 | 50 | 2.4 | 2.2 | 2.7 | 2.8 |
| May | 1.8 | 0.7 | 0.2 | 0.7 | 0 | 100 | 50 | 33 | 0 | 33 | 1.4 | 2.2 | 4.9 | 2.8 |
| | 1.9 | 2.6 | 0.5 | 1.0 | 39 | 89 | 41 | 35 | 39 | 33 | 2.1 | 2.4 | 3.7 | 2.9 |
| June | 1.4 | 2.1 | 1.4 | 1.4 | 50 | 83 | 17 | 22 | 67 | 17 | 1.5 | 2.0 | 3.8 | 1.6 |
| July | 2.5 | 2.5 | 1.8 | 1.4 | 50 | 67 | 55 | 36 | 25 | 50 | 1.2 | 2.4 | 6.4 | 3.1 |
| August | 2.7 | 2.0 | 0.7 | 1.1 | 67 | 60 | 17 | 22 | 67 | 20 | 2.2 | 1.8 | 4.1 | 3.4 |
| | 2.2 | 2.2 | 1.3 | 1.3 | 56 | 70 | 30 | 27 | 53 | 29 | 1.6 | 2.0 | 4.8 | 2.7 |
| September | 2.3 | 2.1 | 0.9 | 1.2 | 75 | 60 | 50 | 33 | 50 | 0 | 1.9 | 1.8 | 4.5 | 2.8 |
| October | 1.1 | 1.6 | 0.7 | 0.2 | 67 | 100 | 60 | 0 | 33 | 0 | 1.6 | 1.6 | 4.2 | 3.0 |
| | 1.7 | 1.8 | 0.8 | 0.7 | 71 | 80 | 55 | 19 | 42 | 0 | 1.8 | 1.7 | 4.4 | 2.9 |
| November | 1.4 | 1.9 | 0.7 | 1.4 | 67 | 50 | 83 | 0 | 67 | 0 | 3.7 | 1.6 | 5.0 | 2.0 |
| December | 2.5 | 2.0 | 1.1 | 1.1 | 40 | 80 | 36 | 0 | 40 | 0 | 1.9 | 1.6 | 2.6 | 2.0 |
| | 2.0 | 2.0 | 0.9 | 1.3 | 54 | 65 | 60 | 0 | 54 | 0 | 2.8 | 1.6 | 3.8 | 2.0 |
| Monthly average | 8.3 | 10.2 | 3.6 | 5.3 | 55 | 78 | 42 | 23 | 48 | 16 | 2.3 | 2.1 | 4.1 | 2.7 |

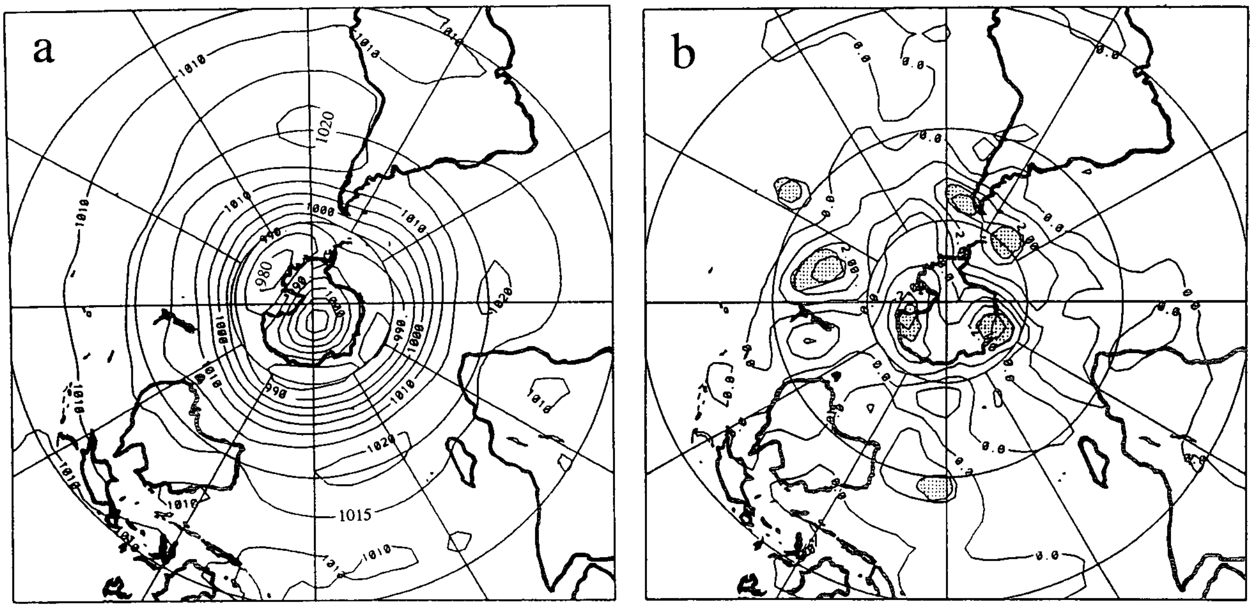


CONTOUR FROM 975 TO 1020 CONTOUR INTERVAL OF 5 hPa

CONTOUR FROM -2.0 TO 1.0 CONTOUR INTERVAL OF 1

FIG. 12. Same as Fig. 11 but for 1984.

termination of cyclogenesis events. Weak cyclones forming near Terra Nova Bay might be missing from the analyses if they did not affect the surrounding stations. If this happened in 1984, the number of cyclones would have been underestimated, and the number of significant cyclones overestimated. Assuming, according to the 1985 and 1988 results, that the number of cyclones is almost the same every year (100–122), and applying these numbers as a total for 1984, it is found that the percentage of significant cyclones could range between 16% and 20%, which agrees with the result in 1988. This isolates 1985 as the year for which the significant cyclones were most frequent and for which the synoptic environment associated with cyclogenesis was somewhat different from that in 1984 and 1988.

Comparison of the three annual hemispheric averages indicates that 1985 has a deeper circumpolar trough, as well as a deeper polar vortex at 500 hPa than 1984 and 1988. This can be noted by the small area enclosed by the 975-hPa isobar to the northeast of the Ross Sea for 1985 (Fig. 13a), which is 5 hPa lower than the last isobar enclosing the quasi-stationary low pressure center for 1988 and 1984 (Figs. 11a and 12a). At 500 hPa (not reproduced), the polar vortex center was enclosed by the 4920 isohypse in 1985, which is 60 gpm lower than the lowest isohypse enclosing the vortex center in 1984 and 1988. Comparison of the 500-hPa field for 1984 and 1988 with 1985 shows stronger westerly winds between 40° and 70°S for 1985. According to Rogers (1983), this should be linked with colder than average temperatures at mainland Antarctic stations and warmer temperatures for peninsula sector stations. Therefore, 1985 should show colder temperatures over the plateau than 1984 and 1988, and in fact, the 1000–500-hPa geopotential thicknesses are slightly lower for 1985. This agrees with Rogers and van Loon (1982), who found that the mean vertical temperature profile over Amundsen–Scott South Pole Station is colder during periods of strong westerlies at 500 hPa than during periods of weak westerlies.

These annual differences are also found by comparing the three annual averages for cyclogenesis days (not shown: Carrasco 1992). A deeper circumpolar trough and polar vortex at 500 hPa are observed for 1985, as well as stronger westerly winds between 40° and 70°S. Thus, 1985 has a distinct synoptic environment around the Antarctic continent. However, because no major differences exist between the annual average and the CEA, the interannual variability of the significant mesoscale cyclones obtained for 1984 and 1988 in comparison to 1985 should be associated with the interannual variation of the large-scale environment. It was mentioned that the comparison of the weekly mesoscale cyclogenesis activity between 1988 and 1985 revealed that the larger activity in 1988 occurred during late summer and autumn with the maximum during late summer (Table 5). The seasonal large-scale average for both years revealed a deeper circumpolar trough and deeper polar vortex at 500 hPa for the late summer season in 1988. This situation reverses for the rest of the year where the circumpolar trough and the 500-hPa polar vortex are deeper during 1985 as shown by the annual averages. On the other hand, the 1000–

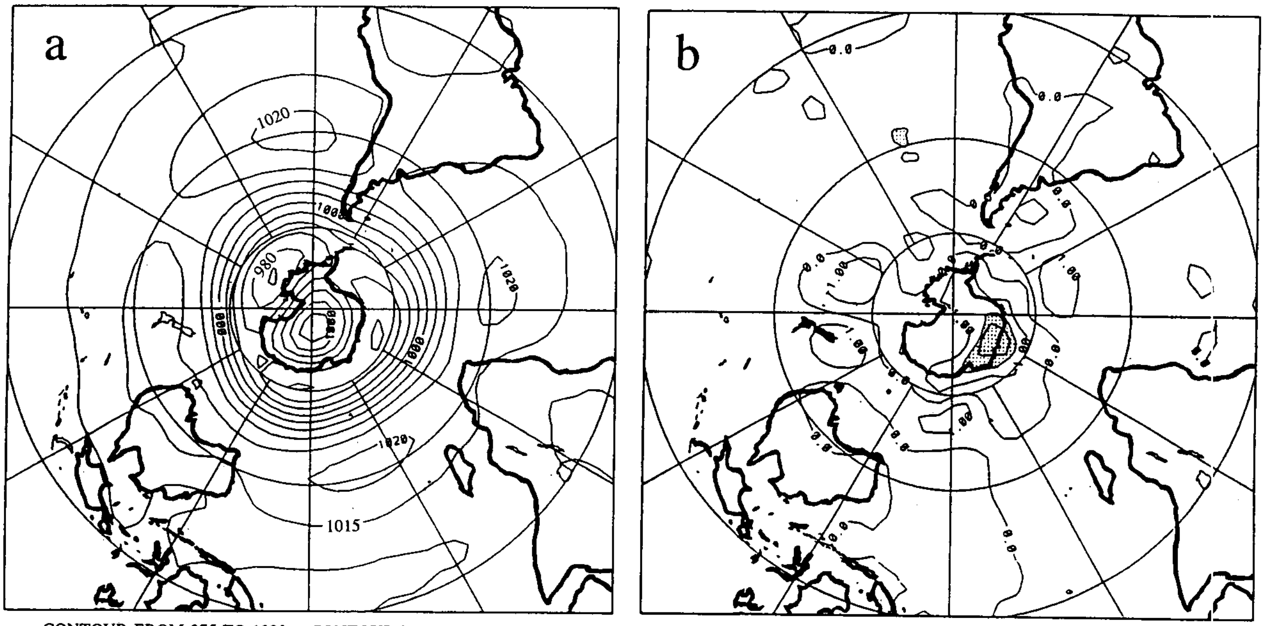


CONTOUR FROM 975 TO 1020 CONTOUR INTERVAL OF 5 hPa

CONTOUR FROM -2.0 TO 1.0 CONTOUR INTERVAL OF 1.

FIG. 13. Same as Fig. 11 but for 1985.

500-hPa geopotential thicknesses are slightly lower for 1985 during the late summer and autumn seasons. This may explain why although late summer season in 1988 shows larger activity, it had fewer significant mesoscale cyclones than 1985. That is, that despite the deeper circumpolar trough and 500 hPa in the summer of 1988, the higher 1000–500-hPa thickness over Antarctica indicates that the katabatic winds were comparatively weaker than for 1985. Thus, although during the summer of 1988 there was more frequent and/or stronger warm-air advection over the Ross Sea, the cold katabatic airflow was less frequent and/or weaker than for 1985, and as a result the percentage of significant mesoscale cyclones was significantly smaller.

Therefore, on average, the larger number of significant mesoscale cyclones in 1985 in relation to 1988 and 1984 can be linked to the simultaneous occurrence of the following:

(a) A deeper circumpolar trough, which in the area near the Ross Sea is manifested as a deeper quasi-stationary synoptic cyclone.

(b) A deeper polar vortex at 500 hPa, which on average was centered over the Ross Sea/Ross Ice Shelf.

(c) Lower geopotential thickness over the plateau, which indicates a colder troposphere.

(d) Stronger westerly winds between 40° and 70°S. This suggests colder air temperatures over the plateau (Rogers 1983; Rogers and van Loon 1982).

## 4. Summary and discussion

The one-year satellite analysis of the spatial distribution of initial mesoscale cyclone appearance shows two areas where cyclones tend to cluster (Figs. 7a–d): one over the southwestern corner of the Ross Sea, and the other near Byrd Glacier. The satellite mesoscale cyclone detection also showed large activity in surrounding areas. Overall, the average size of the mesoscale vortices was under $3 \times 10^2$ km, at least during 1988 and within the study region. This may explain the failure of the operational numerical models to resolve them, as mentioned by Turner et al. (1993b). As with previous studies (Carleton and Carpenter 1989; Carleton and Fitch 1993), most of the mesovortices were of comma-cloud type and were shallow (low cloud signatures associated with them). The trajectories of individual vortices (Figs. 8a–d) confirm these areas as sources for formation of mesoscale cyclones and reveal Marie Byrd Land as a third source of mesoscale cyclones. The latter source may be associated with synoptic-scale storms that decay to the northeast of the Ross Sea. The surface impact of these synoptic storms is the advection of warm air into the interior of the Marie Byrd Land that can interact with cold katabatic winds that converge into the Siple Coast area. This can create boundary layer baroclinic zones. Upper-level cyclonic vorticity maxima associated with the occluded synoptic cyclones may trigger the formation and/or redevelopment of mesoscale cyclones in these baroclinic zones. [See Rasmussen and Zick (1987) for a case in the Northern Hemisphere.]

The integration of AWS regional analyses with the satellite images indicates that about two (one) mesoscale cyclones form each week over the southwestern corner of the Ross Sea (near Byrd Glacier). These results are very similar to those obtained by Bromwich (1991) for 1985, confirming the large mesoscale activity of these two areas. The monthly average duration for all the mesoscale cyclones resolved by the regional sea level analyses was about 25 h, with February and March being the months that have the longest durations; these are also the months that, on average, had the highest maximum intensity of mesoscale cyclones near Terra Nova Bay/Franklin Island (Table 3).

The annual number of significant cyclones found in 1988 is significantly lower than that obtained by Bromwich (1991) in 1985 (Table 5). Also, the duration and maximum intensity are lower for 1988 (Fig. 10). This indicates weaker and less persistent mesoscale cyclones in 1988 than 1985. After reanalyzing the results obtained for 1984 (Bromwich 1991), it was found that 1985 appears to be the year with the largest number of significant mesoscale cyclones, with 1984 being very similar to 1988. These results suggest that although the interannual variability of mesoscale cyclogenesis activity may be small, the percentage of cyclones that acquire major intensity and duration can vary markedly. This was found to be related to the large-scale interannual variation. The deeper quasi-stationary synoptic cyclone to the north of Marie Byrd Land found for 1985 is indicative of more frequent and/or stronger synoptic-scale cyclones moving into and decaying in this area. This suggests that the southwestward warm-air advection associated with these cyclones toward the Ross Sea–Ross Ice Shelf area could be more pronounced during 1985. On the other hand, the fact that 1985 recorded colder temperatures over the plateau than 1984 and 1988 indicates a more intense katabatic wind regime over Antarctica. Businger (1987) studied the synoptic-scale pattern associated with well-developed polar lows (as derived from satellite imagery) over the Gulf of Alaska and the Bering Sea. His superimposed-epoch analysis shows maximum negative sea level pressure anomalies centered over the area where polar lows were observed. The same results were found at 500 hPa and for the 1000–500-hPa geopotential thickness. This synoptic pattern, which supports the development of intense polar lows in the Northern Hemisphere, is different from that found for the Ross Sea–Ross Ice Shelf area. Here, the synoptic anomalies are centered to the northeast of the genesis area of significant mesoscale cyclones.

Bromwich et al. (1993b) calculated the February–April average wind speed at Inexpressible Island, Terra Nova Bay, from 1984 to 1989. The calculations were limited because wind data were unavailable for the remainder of 1984 and 1985; this sharply curtails the characterization of the interannual wind speed variations at this site. Their results indicate stronger katabatic winds in 1985, which may be linked to colder temperatures over the plateau. Dutton and Stone (1991) analyzed recent interannual variations during the fall season of some atmospheric parameters at the South Pole. From their results, it can be seen (see their Fig. 9) that 1985 had colder air temperatures than 1984 and 1988. Stearns and Wendler (1988) and Breckenridge et al. (1993) pointed out that the presence of large wind signatures [dark plumes on infrared satellite image that are revealing the presence of katabatic winds (Bromwich 1989c)] over the Ross Ice Shelf are a manifestation of strong katabatic winds coming down from East Antarctica, and they are associated with a negative potential temperature difference between Dome C and the Ross Ice Shelf. As Breckenridge et al. (1993) noted, these observational results support the suggestion that stronger katabatic winds required a larger than normal supply of cold boundary layer air over the plateau. The barotropic characteristics of the Antarctic troposphere (e.g., Phillpot 1991) means that the free atmosphere was likely colder than usual.

In summary, the large number of significant mesoscale cyclones over the western Ross Sea in 1985 could be caused by 1) more frequent and/or persistent southwestward warm-air advection toward the western Ross Sea associated with synoptic storms moving into and decaying near Marie Byrd Land, and 2) more intense and/or persistent cold katabatic winds blowing into the warmer environment of the Ross Sea. These katabatic winds are the result of cold boundary layer air converging into Reeves and David Glaciers and then propagating across the Ross Sea. The interaction between these two air masses, on the subsynoptic scale, could create stronger baroclinic disturbances over the Terra Nova Bay–Franklin Island area. Above the boundary layer in the free atmosphere, Kutzbach and Schwerdtfeger (1967) showed that there was time-averaged warm-air advection and rising motion over West Antarctica and cold-air advection and sinking motion over East Antarctica. This prevailing tropospheric circulation exhibits similarities with the overall pattern found for significant mesoscale cyclone formation near Terra Nova Bay.

Yasunari and Kodama (1993) studied the intraseasonal variability of katabatic winds at Mizuho Station (70°42′S, 44°20′E, 2230-m elevation), and their relation with the planetary flow regime in the Southern Hemisphere. They found that the strong (weak) katabatic wind phase corresponds to a shallower and broadened (deepened and narrowed) polar vortex with weaker (stronger) westerly winds over the surrounding oceans. The different results of these authors may be due to the location of their site, which is on the opposite side of the continent in relation to the sites located over the Ross Ice Shelf, and Mizuho may not reflect the behavior of the katabatic winds over the Ross Sea–Ross Ice Shelf sector. However, further studies are needed to investigate the katabatic wind behavior on both sides of the continent and its relation to the upper-level flow.

Further studies are also needed to investigate the broadscale environment associated with significant mesoscale cyclone activity over the southwestern Ross Sea. The large-scale average for these events in 1988 and the interannual comparison of the three years revealed a close relation between the intensity of the circumpolar trough/polar vortex and the significant mesoscale cyclones. An ongoing study of the interannual variation of katabatic winds blowing across the Ross Ice Shelf from West Antarctica [defined as katabatic surge (Liu et al. 1994); see also Bromwich et al. (1993a)] that usually are accompanied by katabatic winds from East Antarctica also showed a close relation between katabatic surge frequency and the intensity of the circumpolar trough and polar vortex.

From the present work, as a result of the high frequency of mesoscale cyclone formation, and the number of these that develop into deep circulations, these vortices may no longer be considered unable to significantly perturb the polar vortex. Because mesoscale cyclones form and develop near the katabatic confluence zones adjacent to the coastal margin, they can remove part of the coastal baroclinicity and move it northward. They can feed low-level vorticity into decaying synoptic-scale cyclones, retarding their total dissipation, and/or they can develop into synoptic-scale features (Bromwich 1989b). Therefore, mesoscale cyclones can contribute indirectly to the reduction of the strength of the upper polar vortex. On the other hand, the large mesoscale cyclonic activity observed near Terra Nova Bay and Byrd Glacier for the three years, and the activity found over the Ross Sea and Ross Ice Shelf in this study, provides observational support for the simulated subpolar convergence zone and the secondary cyclogenesis zone found by Tzeng et al. (1993) and Murray and Simmonds (1991), respectively, over the coastline of Antarctica.

Finally, it is also interesting to note that the Darwin and Tahiti pressure anomalies (according with Trenberth and Branstator 1989) indicate that 1984 and 1988 have similar positive anomalies at both stations (about +0.5 hPa). Both years correspond to the first year after the El Niño events of 1982–83 and 1986–87, respectively. On the other hand, 1985 corresponds to the cold phase of the Southern Oscillation (La Niña event) with maximum negative anomalies at both stations (about −0.5 hPa). Carleton and Carpenter (1989) have already found a possible link between the Southern Oscillation and the mesoscale cyclonic activity over the Southern Hemisphere. Their results indicate that the occurrence of mesoscale cyclones during the winter of 1982 (year 0) showed greater activity than the winter of 1981 (year −1) as well as a shift in the spatial location of the maximum occurrence of mesoscale cyclones. However, more studies are needed to investigate any relation between the Southern Oscillation and the mesoscale activity over high southern latitudes.

*Acknowledgments.* This research was sponsored by the Division of Polar Programs of the National Science Foundation through Grants DPP-8816792 and DPP-9117448 to D. H. Bromwich. The satellite imagery was recorded by the U.S. Navy personnel at McMurdo Station and obtained from Robert Whritner of the Arctic and Antarctic Research Center at Scripps Institution of Oceanography (NSF Grant DPP-8815818). The satellite data were processed using the TeraScan software package developed by SeaSpace. We thank the editor, Daniel Keyser, and the two anonymous reviewers for their comments. Also, we thank Zhong Liu for producing the Southern Hemisphere analyses, Beth Daye for the enhancement of the satellite imagery, and John Nagy for drafting Figs. 1, 7, 8, 9, and 10.

## REFERENCES

Breckenridge, C. J., U. Radok, C. R. Stearns, and D. H. Bromwich, 1993: Katabatic winds along the Transantarctic Mountains. *Antarctic Meteorology and Climatology: Studies Based on Automatic Weather Stations, Antarctic Research Series,* Vol. 61, D. H. Bromwich and C. R. Stearns, Eds., Amer. Geophys. Union, 69–92.

Bromwich, D. H., 1986: Boundary layer meteorology of the western Ross Sea. *Antarct. J. U.S.,* **21**(5), 235–237.

——, 1987: A case study of mesoscale cyclogenesis over the southwestern Ross Sea. *Antarct. J. U. S.,* **22**(5), 254–256.

——, 1989a: An extraordinary katabatic wind regime at Terra Nova Bay, Antarctica. *Mon. Wea. Rev.,* **117,** 688–695.

——, 1989b: Subsynoptic-scale cyclone developments in the Ross Sea sector of the Antarctic. *Polar and Arctic Lows,* P. F. Twitchell, E. A. Rasmussen, and K. L. Davidson, Eds., A. Deepak Publishing, 331–345.

——, 1989c: Satellite analyses of Antarctic katabatic wind behavior. *Bull. Amer. Meteor. Soc.,* **70,** 738–749.

——, 1991: Mesoscale cyclogenesis over southwestern Ross Sea linked to strong katabatic winds. *Mon. Wea. Rev.,* **119,** 1736–1752.

——, T. R. Parish, and C. A. Zorman, 1990: The confluence zone of the intense katabatic winds at Terra Nova Bay, Antarctica, as derived from airborne sastrugi surveys and mesoscale numerical modeling. *J. Geophys. Res.,* **95,** 5496–5509.

——, J. F. Carrasco, and C. R. Stearns, 1992: Satellite observations of katabatic wind propagation for great distances across the Ross Ice Shelf. *Mon. Wea. Rev.,* **120,** 1940–1949.

——, ——, Z. Liu, and R.-Y. Tzeng, 1993a: Hemispheric atmospheric variations and oceanographic impacts associated with katabatic surges across the Ross Ice Shelf, Antarctica. *J. Geophys. Res.,* **98,** 13 045–13 062.

——, T. R. Parish, A. Pellegrini, C. R. Stearns, and G. A. Weidner, 1993b: Spatial and temporal characteristics of the intense katabatic winds at Terra Nova Bay, Antarctica. *Antarctic Meteorology and Climatology: Studies Based on Automatic Weather Stations, Antarctic Research Series,* Vol. 61, D. H. Bromwich and C. R. Stearns, Eds., Amer. Geophys. Union, 47–68.

——, Y. Du, and T. R. Parish, 1994: Numerical simulation of winter katabatic winds from West Antarctica crossing Siple Coast and the Ross Ice Shelf. *Mon. Wea. Rev.,* **122,** 1417–1435.

Businger, S., 1987: The synoptic climatology of the polar-low outbreaks over the Gulf of Alaska and Bering Sea. *Tellus,* **39A,** 307–325.

——, and R. J. Reed, 1989: Polar lows. *Polar and Arctic Lows,* P. F. Twitchell, E. A. Rasmussen, and K. L. Davidson, Eds., A. Deepak Publishing, 3–45.

Carleton, A. M., 1979: A synoptic climatology of satellite-observed extratropical cyclone activity for the Southern Hemisphere winter. *Arch. Meteor. Geophys. Bioklimatol.,* **B27,** 265–279.

——, 1981a: Ice–ocean–atmosphere interactions at high southern latitudes in winter from satellite observation. *Aust. Meteor. Mag.*, **29**, 183–195.

——, 1981b: Monthly variability of satellite-derived cyclone activity for the Southern Hemisphere winter. *J. Climatol.*, **1**, 21–38.

——, 1983: Variation of Antarctic sea ice conditions and relationship with Southern Hemisphere cyclonic activity, winters 1973–77. *Arch. Meteor. Geophys. Bioklimatol.*, **B32**, 1–22.

——, and D. A. Carpenter, 1989: Intermediate-scale sea-ice–atmosphere interactions over high southern latitudes in winter. *Geojournal*, **18**, 87–101.

——, and ——, 1990: Satellite climatology of "polar lows" and broadscale climatic associations for the Southern Hemisphere. *Int. J. Climatol.*, **10**, 219–246.

——, and M. Fitch, 1993: Synoptic aspects of Antarctic mesocyclones. *J. Geophys. Res.*, **98**, 12 997–13 018.

Carrasco, J. F., 1992: A mesoscale cyclogenesis study adjacent to the Pacific coast of Antarctica. M.S. thesis, Atmospheric Sciences Program, The Ohio State University, 179 pp.

——, and D. H. Bromwich, 1991: A case study of katabatic wind-forced mesoscale cyclogenesis near Byrd Glacier. *Antarct. J. U.S.*, **26**(5), 258–261.

——, and ——, 1992: Mesoscale cyclogenesis over the southeastern Pacific Ocean. *Antarct. J. U.S.*, **27**(5), 289–291.

——, and ——, 1993a: Mesoscale cyclogenesis dynamics over the southwestern Ross Sea, Antarctica. *J. Geophys. Res.*, **98**, 12 973–12 995.

——, and ——, 1993b: A katabatic wind–forced mesoscale cyclone development over the Ross Ice Shelf near Byrd Glacier during summer. *Antarct. J. U.S.*, **28**(5), 285–287.

Dutton, E. G., and R. S. Stone, 1991: Recent interannual variations in solar radiation, cloudiness, and surface temperature at the South Pole. *J. Climate*, **4**, 848–868.

Fitch, M., and A. M. Carleton, 1992: Antarctic mesoscale regimes from satellite and conventional data. *Tellus*, **44A**, 180–196.

Forbes, G. S., and W. D. Lottes, 1985: Classification of mesoscale vortices in polar airstreams and the influence of the large scale environment on their evolution. *Tellus*, **37A**, 132–155.

Guymer, L. B., 1986: Procedures and concepts used in Southern Hemisphere analyses at WMC Melbourne. *Extended Abstracts, Second Int. Conf. on Southern Hemisphere Meteorology*, Wellington, New Zealand, Amer. Meteor. Soc., 10–16.

Heinemann, G., 1990: Mesoscale vortices in the Weddell Sea region (Antarctica). *Mon. Wea. Rev.*, **118**, 779–793.

James, I. N., 1989: The Antarctic drainage flow: Implications for hemispheric flow on the Southern Hemisphere. *Antarct. Sci.*, **1**, 279–290.

Keller, L. M., G. A. Weidner, C. R. Stearns, and M. F. Sievers, 1989: Antarctic automatic weather station data for the calendar year 1988. Department of Meteorology, University of Wisconsin—Madison, 329 pp. [Available from Dept. of Atmospheric and Oceanic Sciences, 1225 W. Dayton St., Madison, WI 53706.]

Kutzbach, G., and W. Schwerdtfeger, 1967: Temperature variations and vertical motion in the free atmosphere over Antarctica in the winter. Polar Meteorology, WMO Tech. Note No. 87, 225–248.

Liu, Z., D. H. Bromwich, and J. F. Carrasco, 1994: Interannual variation of katabatic surges across the Ross Ice Shelf, Antarctica. *Sixth Conf. on Climate Variations*, Nashville, TN, Amer. Meteor. Soc., 245–249.

Lyons, S. W., 1983: Characteristics of intense Antarctic depressions. Preprints, *First Int. Conf. on Southern Hemisphere Meteorology*, Sao Jose Dos Campos, Brazil, Amer. Meteor. Soc., 238–240.

Mansfield, D. A., 1974: Polar lows: The development of baroclinic disturbances in cold air outbreaks. *Quart. J. Roy. Meteor. Soc.*, **100**, 541–554.

Murray, R. J., and I. Simmonds, 1991: A numerical scheme for tracking cyclone centers from digital data. Part II: Application to January and July general circulation model simulations. *Aust. Meteor. Mag.*, **39**, 167–180.

Naval Polar Oceanography Center, 1989: Antarctic ice charts 1988–1989. Naval Polar Oceanography Center.

O'Connor, W. P., D. H. Bromwich, and J. F. Carrasco, 1994: Cyclonically forced barrier winds along the Transantarctic Mountains near Ross Island. *Mon. Wea. Rev.*, **122**, 137–150.

Parish, T. R., and D. H. Bromwich, 1987: The surface windfield over the Antarctic ice sheets. *Nature*, **328**, 51–54.

——, and ——, 1989: Instrumented aircraft observations of the katabatic wind regime near Terra Nova Bay. *Mon. Wea. Rev.*, **117**, 1570–1585.

——, and ——, 1991: Continental-scale simulation of the Antarctic katabatic wind regime. *J. Climate*, **4**, 135–146.

Phillpot, H. R., 1991: The derivation of 500 hPa height from automatic weather station surface observations in the Antarctic continental interior. *Aust. Meteor. Mag.*, **39**, 79–86.

Rasmussen, E., 1981: An investigation of a polar low with spiral cloud structure. *J. Atmos. Sci.*, **38**, 1785–1792.

——, and C. Zick, 1987: A subsynoptic vortex over the Mediterranean with some resemblance to polar lows. *Tellus*, **39A**, 408–425.

Rogers, J. C., 1983: Spatial variability of Antarctic temperature anomalies and their association with the Southern Hemisphere atmospheric circulation. *Ann. Assoc. Amer. Geogr.*, **73**, 502–518.

——, and H. van Loon, 1982: Spatial variability of sea level pressure and 500 mb height anomalies over the Southern Hemisphere. *Mon. Wea. Rev.*, **110**, 1375–1392.

Schwerdtfeger, W., 1970: The climate of the Antarctic. *Climate of the Polar Regions, World Survey of Climatology*, Vol. 14, S. Orvig, Ed., Elsevier, 253–355.

——, 1984: *Weather and Climate of the Antarctic*. Elsevier, 261 pp.

Shanmin, C., Z. Linyu, and L. Changgui, 1990: Statistical analysis of cyclone tracks in western Antarctic region. *Acta Meteorol. Sin.*, **4**, 74–80.

Stearns, C. R., and G. Wendler, 1988: Research results from Antarctic automatic weather stations. *Rev. Geophys.*, **26**, 45–61.

Streten, N. A., and A. J. Troup, 1973: A synoptic climatology of satellite-observed cloud vortices over the Southern Hemisphere. *Quart. J. Roy. Meteor. Soc.*, **99**, 56–72.

Taljaard, J. J., 1967: Development, distribution and movement of cyclones and anticyclones in the Southern Hemisphere during the IGY. *J. Appl. Meteor.*, **6**, 973–987.

Trenberth, K. E., 1991: Storm tracks in the Southern Hemisphere. *J. Atmos. Sci.*, **48**, 2159–2178.

——, and G. W. Branstator, 1989: Global circulation anomalies during 1988. *Extended Abstracts, Third Int. Conf. on Southern Hemisphere Meteorology and Oceanography*, Buenos Aires, Argentina, Amer. Meteor. Soc., 110–115.

Turner, J., and J. P. Thomas, 1992: Southern Ocean weather systems in satellite imagery and operational numerical analyses. *Proc. Sixth Conf. on Satellite Meteorology and Oceanography*, Atlanta, GA, Amer. Meteor. Soc., 149–152.

——, T. A. Lachlan-Cope, D. E. Warren, and C. N. Duncan, 1993a: A mesoscale vortex over Halley Station, Antarctica. *Mon. Wea. Rev.*, **121**, 1317–1336.

——, ——, and J. P. Thomas, 1993b: A comparison of Arctic and Antarctic mesoscale vortices. *J. Geophys. Res.*, **98**, 13 019–13 034.

Tzeng, R.-Y., D. H. Bromwich, and T. R. Parish, 1993: Present-day Antarctic climatology of the NCAR Community Climate Model version 1. *J. Climate*, **6**, 205–226.

Van Woert, M. L., R. H. Whritner, D. E. Waliser, D. H. Bromwich, and J. C. Comiso, 1992: ARC: A source of multisensor satellite data for polar science. *Eos, Trans. Amer. Geophys. Union*, **73**(6), 65, 75–76.

Warren, D. E., and J. Turner, 1989: Studies of Antarctic mesoscale systems using satellite imagery and sounder data. *Polar and Arctic Lows*, P. F. Twitchell, E. A. Rasmussen, and K. L. Davidson, Eds., A. Deepak Publishing, 389–400.

Yasunari, T., and S. Kodama, 1993: Intraseasonal variability of katabatic wind over East Antarctica and planetary flow regime in the Southern Hemisphere. *J. Geophys. Res.*, **98**, 13 063–13 070.